People`s Democratic Republic of Algeria
Ministry of Higher Education and Scientific Research
University of Echahid Hamma Lakhdar - El Oued
Faculty of Technology
Department of Process Engineering & Petrochemistry

Dissertation

ACADEMIC MASTER

Domain: Science and Technology

Division: Chemical Engineering

Specialty: Chemical Engineering

Presented by:

Chaar Hamza

Omar Falah

Khachana Kaiss

Entitled:

Assessing the anticorrosive activity of some organic molecules containing heteroatoms

Dissertation Submitted in Partial Fulfillment of the Requirements for the Master Degree in Chemical Engineering

Publicly defended in: 28/05/2025

Board of Examiners:

Dr. Guemari Fathi	**Chairman**
Dr. Hachani Salah Eddine	**Supervisor**
Dr. Benamor Mohamed Larbi	**Examiner**

Academic Year: 2024/2025

Abstract:

Density Functional Theory (DFT) was employed to investigate the global reactivity descriptors and Mulliken charge distribution, along with structure–activity relationship (SAR) analysis and molecular dynamics (MD) simulations. These computational methods were applied to examine how the electronic properties of two compounds namely 2-thiophene carboxylic acid (TC1) and 2-thiophene carboxylic acid hydrazide relate to their effectiveness in inhibiting the corrosion of carbon steel in an acidic environment. The results from the reactivity descriptors, SAR analysis, and MD simulations aligned well with experimental findings, confirming their corrosion inhibition performance. Furthermore, the Mulliken charge analysis provided insight into the reactive sites within the molecules, identifying the atoms most likely involved in electron transfer processes.

Keywords: DFT, global reactivity parameters, Mulliken charges, SAR, MD, TC1, TC2.

ملخص:

استُخدمت نظرية الكثافة الوظيفية (DFT) لدراسة مُوَصِّفات التفاعلية الشاملة وتوزيع شحنات موليكن، بالإضافة إلى تحليل علاقة البنية بالنشاط (SAR) ومحاكاة الديناميكيا الجزيئية (MD). طُبِّقت هذه الطرق الحسابية لدراسة كيفية ارتباط الخصائص الإلكترونية لمركبين، وهما حمض 2-ثيوفين الكربوكسيلي (TC1) وهيدرازيد حمض 2-ثيوفين الكربوكسيلي، بفعاليتهما في تثبيط تآكل الفولاذ الكربوني في بيئة حمضية. وقد توافقت نتائج مُوَصِّفات التفاعلية، وتحليل علاقة البنية بالنشاط، ومحاكاة الديناميكيات الجزيئية بشكل جيد مع النتائج التجريبية، مؤكدةً أداءهما في تثبيط التآكل. علاوةً على ذلك، وفّر تحليل شحنات موليكن فهمًا أعمق للمواقع التفاعلية داخل الجزيئات، مُحددًا الذرات التي يُحتمل تورطها في عمليات نقل الإلكترون.

الكلمات المفتاحية: نظرية الكثافة الوظيفية، معاملات التفاعلية الشاملة، شحنات موليكن، SAR، MD، TC1، TC2.

Dedication

In the Name of God, the Most Gracious, the Most Merciful Praise be to ALLAH, by whose grace good deeds are accomplished. Peace and blessings be upon our Master Muhammad, the best of ALLAH's creation, and upon all his family and companions.

To my dear parents, my support after ALLAH, may ALLAH reward you both on my behalf. I ask Him to place this effort in your scale of good deeds.

To my brothers and my sisters

To my best friends, to my teachers in the university

I dedicated this fruitful work

Acknowledgements

First and foremost, we would like to express our deepest gratitude to ALLAH (s.w.t) for granting us perseverance and patience throughout this Master's journey.

We are profoundly grateful to Dr. Hachani Salah Eddine for his unwavering support and timely corrections when we needed them most during our research.

We would also like to extend our sincere thanks to Dr. Guermari Fathi, and Dr. Ben Amor Mohamed Larbi for agreeing to discuss our thesis and provide invaluable feedback.

Lastly, but certainly not least, we are immensely thankful to our family for their unwavering support. Thank you for always being there for us and offering your help whenever we needed them.

Table of contents

Chapter 2: Quantum computational methods

Chapter 3: Results and discussion

List of figures

List of tables

List of abbreviations

DFT: Density Functional Theory

HF: Hartree Fock

GGA: Generalized Gradient Approximation

LDA: Local Density Approximation

PBE: Pedrew-Bruk-Ernezrhof

B3LYP: Becke, 3-parameter, Lee–Yang–Parr

HOMO: Highest Occupied Molecular Orbital

LUMO: Lowest Unoccupied Molecular Orbital

SAR: Structure-Activity Relationship

General introduction

General introduction

Carbon steel, a type of iron alloy containing between 0.12% and 2% carbon, is commonly used in the construction of piping and valves for refineries and petrochemical facilities. Its popularity is largely due to its cost-effectiveness. However, in offshore environments, carbon steel is vulnerable to corrosion caused by harsh substances like carbon dioxide (CO_2) and hydrogen sulfide (H_2S) found in oil and gas, which can result in significant financial impacts [1,2].

An effective approach to protecting carbon steel involves the incorporation of organic molecules as corrosion inhibitors. These molecules have molecular structures containing heteroatoms (N, P, S, and O), conjugated bonds, and aromatic rings. The adsorption of such compounds onto the metal surface has proven to be an excellent means of protection [3,4]. By using these corrosion inhibitors, the adverse effects of aggressive environments on aluminum can be mitigated, thus ensuring the preservation of its integrity and longevity.

Laboratory techniques, including electrochemical impedance spectroscopy (EIS), gravimetric analysis, and scanning electron microscopy (SEM), serve as the primary means of experimental investigation of the anticorrosion activity of the aforementioned chemical species. However, these techniques have certain limitations. They can be expensive, time-consuming, not always readily available, and provide insufficient depth to fully understand the phenomenon under study and its associated mechanisms [5].

Advances in computer technology have paved the way for the use of computational chemistry as a powerful tool to better understand ambiguities encountered in experimental results [6]. By exploiting the capabilities of computational chemistry, a more comprehensive understanding of corrosion processes and associated mechanisms can be achieved, thus offering valuable contributions to the field of corrosion research.

Density functional theory (DFT) approaches have proven very effective in the field of computational chemistry. By using DFT-based global reactivity descriptors, it becomes possible to elucidate the underlying reasons for the order of inhibition efficiency observed during experimental testing of the compounds studied. Furthermore, using Fukui function analyses, the specific atoms involved in electron transfer during the inhibition process can be precisely identified and characterized [7]. These results highlight the significant contributions of DFT methodologies in understanding the complex mechanisms governing the inhibition

process and provide valuable information on the electronic properties and reactivity of the tested compounds.

The Structure-Activity Relationship (SAR) analysis plays a crucial role in the development of corrosion inhibitors, aiming to establish a quantitative link between the molecular structure of inhibitor compounds and their effectiveness in preventing metal corrosion. By examining the structural features of these compounds, SAR analysis allows for the prediction of their inhibition efficiency. As a result, it becomes an essential tool in the careful design and optimization of corrosion inhibitors [7].

Molecular Dynamics (MD) simulation has become an essential tool in corrosion inhibition research, offering valuable insights into the molecular interactions and mechanisms at play between corrosion inhibitors and metal surfaces.

In a study, the potential of 2-thiophene carboxylic acid (TC1) and 2-thiophene carboxylic acid hydrazide (TC2) to protect carbon steel against corrosion in acidic media was extensively investigated. The results revealed that these two tested compounds exhibit exceptional inhibitory properties, effectively protecting carbon steel from corrosion. Furthermore, the comparison of their inhibition efficiencies demonstrated that TC2 outperforms TC1, indicating that it provides superior corrosion protection for aluminum alloy substrates [8].

The aforementioned research lacks a comprehensive theoretical background to explain the complex experimental observations previously reported. In this current scientific contribution, density functional theory (DFT) calculations and structure-activity relationship (SAR) analyses were used to fully understand the relationship between the anticorrosive activity of the thiophene derivatives studied and their electronic properties at the molecular level.
This dissertation represents a theoretical study based on DFT and SAR calculations to provide an explanation of the inhibition efficiency at the molecular level. This manuscript is structured around three main chapters:

- The first chapter presents a state-of-the-art review of corrosion and protection methods.
- The second chapter details the quantum computational methods, global chemical reactivity, local chemical reactivity, and the software used in this study.
- The third chapter presents the computational procedure and discusses the various theoretical results obtained.

Chapter 1: State-of-the-art review of corrosion and protection methods

1.1. Introduction:

The first chapter provides general information about the phenomenon of corrosion, its various impacts, its forms, the parameters that influence corrosion, and experimental methods for studying this problem. Methods for combating and preventing corrosion are then detailed here. This chapter will be achieved with a conclusion.

1.2. Definition of corrosion:

Corrosion is a natural chemical process that occurs when metallic materials interact with their environment and undergo gradual degradation or deterioration. It is defined as the deterioration of metals and their alloys caused by chemical reactions with corrosive factors such as oxygen, moisture, acids, bases, or other chemicals present in the environment [9].

1.3. Corrosion modes:

1.3.1. Chemical corrosion:

Chemical corrosion occurs when a metal undergoes a chemical reaction with corrosive substances without requiring a complete electrical circuit. This can include corrosion by aggressive chemicals such as strong acids or strong bases [10].

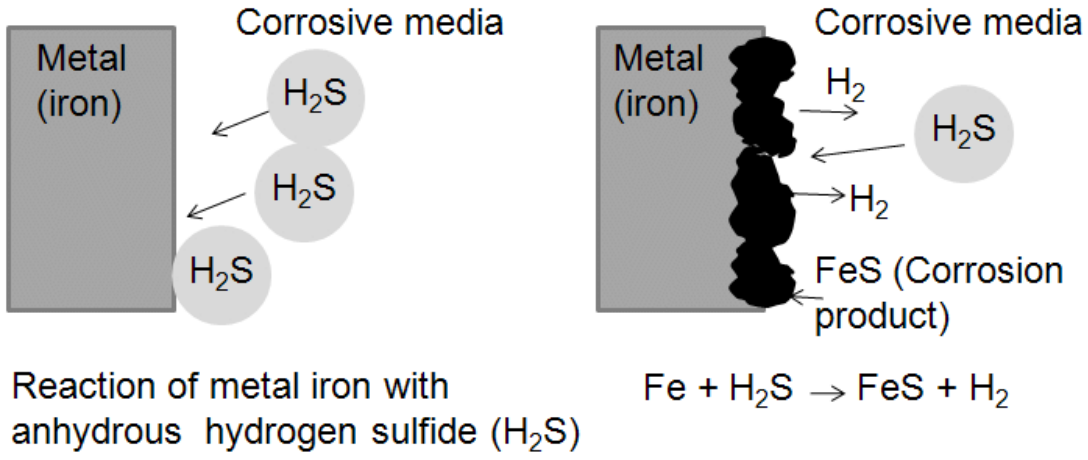

Figure 1.1: Chemical corrosion mechanism of iron metal by hydrogen sulfide acid (H_2S).

1.3.2. Electrochemical corrosion:

This is a corrosion phenomenon that manifests itself through electrochemical reactions between a metallic material, an electrolyte (usually an aqueous solution), and a complete

electrical circuit. It occurs as soon as a heterogeneity or irregularities exist in one of the components of the couple formed by the metal and the reagent, thus leading to the creation of small electrochemical structures, such as batteries or micro-batteries (anodes and cathodes), which arise in the same region of the metal structure [11].

1.3.3. Bacterial corrosion:

Also called microbiological corrosion, is caused by the action of microorganisms such as bacteria, algae, or fungi in the presence of a corrosive environment. These microorganisms can colonize the surface of a metallic material and promote corrosive chemical reactions that accelerate the degradation of the metal. It can occur under various conditions, including industrial cooling systems, pipes, tanks, and other metallic infrastructure in contact with water or liquids [12].

Figure 1.2: Metal corroded by bacteria.

1.4. Forms of corrosion:

1.4.1. Uniform corrosion:

This is characterized by uniform degradation over the entire surface of the material. It occurs when the metal is exposed to a corrosive environment, generally in the presence of moisture and oxygen. It can be easily controlled by monitoring weight loss or reducing the thickness of the metal [13].

Figure 1.3: Metal affected by uniform corrosion.

1.4.2. Pitting corrosion:

Also called localized corrosion, it is characterized by attacks located on specific areas on the surface of a metallic material by certain anions, particularly halides (chlorides, etc.). It results in the creation of small perforations, cavities, or holes, often located in specific areas of the material [14].

Figure 1.4: Metal affected by pitting corrosion.

1.4.3. Galvanic corrosion:

Galvanic corrosion occurs when there is electrical contact between two dissimilar metals in a conductive environment, causing an electrochemical reaction. Each metal has specific electrochemical properties, including corrosion potential. When they come into contact, one becomes the anode and the other the cathode. The anode is the more reactive metal, and corrosion occurs on its surface. The cathode is the less reactive metal, and remains relatively protected [15].

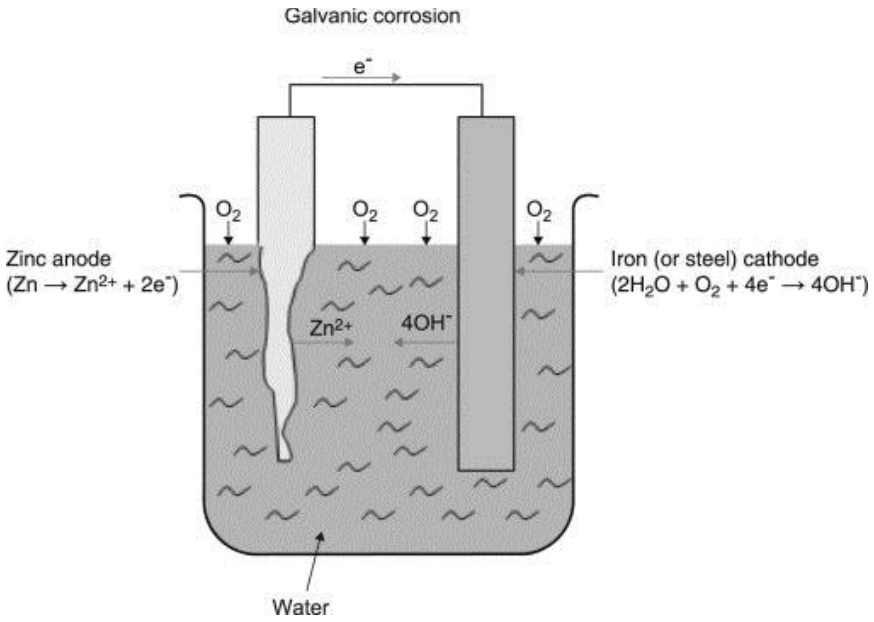

Figure 1.5: Galvanic corrosion between zinc and iron in aqueous environment.

1.4.4. Intergranular corrosion:

Corrosion occurs along grain boundaries or interfaces between grains of a metallic material. Intergranular corrosion can weaken the bonds between grains, which can cause the material to disintegrate and crack along the grain boundaries. Crevice corrosion: Crevice corrosion occurs in crevices or spaces between two or more joined metals. This type of attack is often associated with small volumes of immobile solution generated by perforations, the surfaces of joints, lap joints, surface deposits, and crevices under bolt and rivet heads [15].

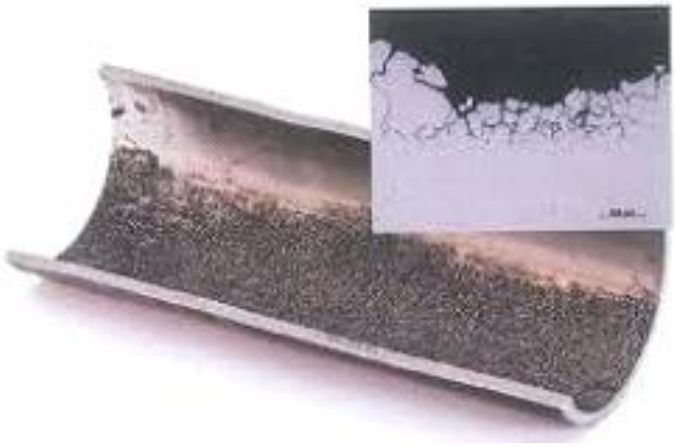

Figure 1.6: Metal affected by intergranular corrosion.

1.4.5. Selective corrosion:

Selective corrosion, also called selective dissolution corrosion, specifically affects one of the elements in a homogeneous alloy, or one of the phases if the alloy is multiphasic, while the other elements remain intact. This phenomenon results in the formation of pores in the metal and a reduction in its strength [16].

Figure 1.7: Metal affected by selective corrosion.

1.5. Negative impacts of corrosion:

Corrosion has major repercussions on several levels including industry, the economy, and the environment. It impacts in these three areas [17]:

- Corrosion seriously affects metal structures including bridges, pipelines, factories, reservoirs, etc.), leading to cracks, leaks, or collapses.
- It can cause machinery or industrial processes to shut down, affecting productivity.
- Corroded equipment becomes dangerous for employees, with an increased risk of accidents.
- Corrosion requires regular inspections, frequent repairs, and sometimes a complete component replacement.
- Purchase of resistant materials, surface treatment, protective coatings, equipment maintenance and replacement.
- Corrosion can cause a production downtime, business interruption, compensation for accidents or environmental damage.
- Corroded assets lose their market value.
- According to the National Association of Corrosion Engineers (NACE), corrosion costs approximately 3 to 4% of global GDP each year.
- Corroded structures such as pipelines can release harmful substances into the environment (hydrocarbons, chemicals, etc.).
- The manufacturing and replacement of corroded parts increases the demand for raw materials (steel, rare metals).
- The production of new materials to replace those destroyed by corrosion leads to increased greenhouse gas emissions.
- Leaks caused by corrosion can kill local flora and fauna.

In the light of previous point we can conclude that corrosion is a pervasive problem with serious consequences. It harms the safety of industrial infrastructure, weighs heavily on the finances of companies and governments, and causes considerable environmental damage. Proactive management of corrosion through prevention, research, and innovation is essential to minimize these impacts.

1.6. Corrosion protection:

The methods of protection and prevention against corrosion are as follows:

1.6.1. Protection by coating:

The structure to be protected is isolated from the corrosive environment using coatings, which may be metallic or non-metallic [18].

1.6.1.1. Metallic coatings:

Metallic coatings are commonly used to protect steel, especially against atmospheric corrosion. Based on their behavior, they are categorized as [19]:

- Noble coatings where the coating metal is nobler than the base metal for example: Nickel or copper coating on steel.
- Sacrificial coatings where the coating metal is less noble than the base metal for example: Galvanization (zinc coating on steel).

1.6.1.2. Non-Metallic coatings:

These coating form a semi-impermeable barrier between the metal surface and the environment. They include:

- Bitumen-based coatings for buried structures.
- Polymeric coatings such as rubber.
- Paints and varnishes.
- Conversion layers.
- Cement-based layers used in civil engineering [20].

1.6.2. Electrochemical protection:

1.6.2.1. Cathodic protection:

The metal is maintained at a sufficiently negative potential so that a reduction current flows, preventing oxidation. The typical reaction is water reduction to hydrogen gas. This method can be achieved in two ways [21]:

• Using a sacrificial anode (a more electronegative metal), directly connected to the protected structure in the same electrolyte.

• Using an impressed current system, where a direct current power supply connects the negative pole to the metal and the positive pole to an auxiliary anode.

1.6.2.2. Anodic protection:

This involves applying a slightly positive potential to the metal, just above its passivation point. It is typically used with naturally passivating materials, such as stainless steel [22].

1.6.3. Protection using corrosion inhibitors:

Protection by corrosion inhibitors involves adding chemical compounds at low concentrations either as a permanent or temporary solution (during storage, cleaning, or acid pickling). The used inhibitor slows or stops corrosion without affecting the physical or chemical properties of the metal, especially its mechanical strength [23].

1.6.3.1. Properties of corrosion inhibitors:

In general, a good corrosion inhibitor should:

1. Reduce the metal's corrosion rate without affecting its physical or mechanical properties.
2. Be stable in the presence of other components in the environment, especially oxidizing agents.
3. Be thermally stable at operating temperature.
4. Be effective at low concentrations.
5. Be non-toxic and comply with safety/environmental regulations.
6. Be cost-effective.

1.6.3.2. Classification of corrosion inhibitor:

The corrosion inhibitors can be classified using different criteria as following [24]:

1.6.3.2.1. Classification according to the nature of the inhibitor:

1.6.3.2.1.1. Organic inhibitors:

Organic inhibitors are generally made from by-products of the petroleum industry. They comprise a non-polar, hydrophobic part, consisting of one or more hydrocarbon chains and a polar, hydrophilic part, consisting of one or more functional groups: amine ($-NH_2$), hydroxyl (-OH), mercapto (-SH), phosphonate ($-PO_3H_2$), sulfonate ($-SO_3H$), carboxyl (-COOH) and their derivatives.

Organic inhibitors are generally used in acidic environments; however, due to their ecotoxicity, they are increasingly used in neutral/alkaline environments. Organic molecules are destined for more than certain development as corrosion inhibitors: their use is currently preferred to that of inorganic inhibitors mainly for ecotoxicity reasons. The inhibitory action of these organic compounds is linked to the formation (by adsorption) of a more or less continuous barrier, but of finite thickness, which prevents access of the solution to the metal. Organic compounds used as inhibitors must possess at least one heteroatom serving as an

active center for their attachment to the metal, such as nitrogen (amines, amides, imidazolines, triazoles, etc.), oxygen (acetylenic alcohols, carboxylates, oxadiazoles, etc.), sulfur (thiourea derivatives, mercaptans, sulfoxides, thiazoles, etc.), or phosphorus (phosphorates).

One limitation in the use of these products may be the increase in temperature, as organic molecules are often unstable at high temperatures. The molecule binds to the surface through its functional group, while its larger, non-polar portion partially blocks the active surface. Other structural parameters that can influence the effectiveness of inhibitors include:

- The molecular area of the inhibitor projected onto the metal surface. This projection depends on the different arrangement possibilities of organic ions or molecules at the metal/solution interface [25].
- The influence exerted by molecular weight [26].
- The importance of molecular configuration, descriptors of the molecule, namely HOMO energy, LUMO energy, and dipole moment μ…) [27].

- The influence of the nature of the substituent [28].

1.6.3.2.1.2. Mineral inhibitors

Mineral inhibitors are used in neutral/alkaline media but rarely in acidic media. It is often their dissociation products (anion or cation) that are effective as corrosion inhibitors. The main inhibitory anions are XO-type oxoanions such as chromates, phosphates, molybdates, nitrates, nitrites, silicates, etc. [29-31] and among the inhibitory cations we find mainly Ca^{2+} and Zn2+ ions and those which form insoluble salts with certain anions such as hydroxyl OH. Mineral inhibitors are used less and less due to their toxicity. Their use is limited to certain closed-circuit systems [32,33]. The number of molecules in use today is becoming increasingly limited, because most of the effective products have a harmful side for the environment. However, new organic complexes of chromium III and other cations (Zn^{2+}, Ca^{2+}, Mg^{2+}, Mn^{2+}, ….Sr^{2+}, Al^{3+}, Zr^{2+}, Fe^{2+}….) have been developed that are effective against corrosion and non-toxic [34].

1.6.3.2.2. Classification according to the mechanism of action

Depending on the reaction mechanism, inhibition is distinguished by: Adsorption, Passivation, Precipitation or Elimination of the corrosive agent. There is no single mode of action for corrosion inhibitors. However, and regardless of the exact mechanism by which each inhibitor acts under the conditions in which it is placed, there are a number of basic considerations that apply to all inhibitors.

1.6.3.2.2.1. Electrochemical mechanism of action

This classification of inhibitors takes into account the electrochemical nature of liquid-phase corrosion, which involves at least two reactions:

- An anodic reaction of metal dissolution (oxidation reaction):

$$M \rightarrow M^{n+} + n\, e^-$$

Example: $Fe \rightarrow Fe^{2+} + n\, e^-$

- A cathodic reaction of reduction of an oxidant in the solution:

$$H^+ + e^- \rightarrow 1/2\ H_2 \text{ (non-aerated acidic medium)}$$

Or: $O_2 + 4H^+ + 4\, e^- \rightarrow 2\ H_2O$ (aerated acidic medium)

The role of the inhibitor will necessarily be to reduce the rate of one of the two reactions, and in some cases both simultaneously. If the inhibitor slows the oxidation reaction by blocking the anodic sites (the site of metal oxidation), it is called an anodic inhibitor. Similarly, if the inhibitor slows the reduction reaction by blocking the cathodic sites (the site of dissolved oxygen reduction in an aerated environment or the site of H^+ proton reduction in an acidic environment), it is called a cathodic inhibitor. Mixed inhibitors act to reduce the rate of both the anodic and cathodic reactions [35].

The inhibitor's action can be conceived as:

- The interposition of a barrier between the metal and the corrosive environment. In the case of acidic environments, the role of adsorption of the compound on the surface will be essential, strengthening a pre-existing barrier, generally the oxide or hydroxide layer formed naturally in a neutral or alkaline environment. This strengthening may consist of an extension of the oxide to the surface, or the precipitation of salts in weak areas of the oxide: these salts are corrosion products (reactions with metal cations).
- The formation of a barrier through interaction between the inhibitor and one or more species in the corrosive medium: this type of mechanism is also specific to neutral or alkaline environments. Considering these general concepts, it becomes clear that the mechanism of action of an inhibitor can be considered from two perspectives: a "mechanism" aspect (intervention in the fundamental processes of corrosion) and a

"morphology" aspect (intervention of the inhibitor molecule in the inter-phase structure).

1.6.3.2.2.2. Interphase Mechanisms of Action

Depending on the mode of attachment to the metal surface, two types of inhibitors are distinguished: adsorption or "interface" inhibitors and so-called "interphase" inhibitors. The former are more commonly observed in acidic environments and act by forming one- or two-dimensional films of the molecules through adsorption on the metal surface, while the latter are specific to neutral or alkaline environments and form three-dimensional films that incorporate the dissolution products of the substrate.

1.6.3.2.2.3. Adsorption of inhibitor molecules on the metal surface

Corrosion can be slowed by the adsorption of an inhibitor on the metal surface. Inhibitors acting by adsorption are generally organic inhibitors. They prevent the action of the aggressive environment by attaching to the metal surface. Their attachment is primarily achieved through the active function of the inhibitor; however, polar components can also be adsorbed. Between the adsorbed species and the metal surface, there are two types of bonds: electrostatic bonding and chemical bonding, thus two distinct types of adsorption: physisorption and chemisorption.

The former, also called physical adsorption, preserves the identity of the adsorbed molecules; three types of forces must be distinguished: Dispersion forces (Van der Waal, London), which are always present; Polar forces, resulting from the presence of an electric field; Hydrogen bonds due to hydroxyl or amine groups. Chemisorption, on the other hand, consists of the sharing of electrons between the polar part of the molecule and the metal surface, which leads to the formation of much more stable chemical bonds because they are based on higher binding energies. The electrons come mainly from the unpaired doublets of the inhibitor molecules such as O, N, S, P, etc. (all these atoms are distinguished from the others by their high electronegativity). Chemical adsorption is accompanied by a profound modification of the distribution of electronic charges of the adsorbed molecules, and often presents an irreversible mechanism [34].

The degree of inhibition depends on the balance between dissolved and adsorbed species. Such a balance is expressed by one of the adsorption isotherms. The effectiveness of inhibition increases in the following order [35, 38]: O < N < S < Se < P

1.6.3.2.2.4. Inhibition by passivation:

Inhibitors acting by passivation are generally mineral inhibitors. They cause spontaneous passivation of the metal by reinforcing the oxide layer naturally formed on the metal surface. They are reduced on the pores of the more or less protective oxide/hydroxide layer that naturally forms on the metal surface. The chromate ion is one of the most effective passivating inhibitors, but its carcinogenic nature and high toxicity significantly limit its use. Buffering agents, which increase the pH near the metal surface, can also promote passivation in certain cases.

1.6.3.2.2.5. Surface film formation by precipitation:

Precipitation inhibitors cause the formation of a surface film consisting of mineral salts or poorly soluble organic complexes formed during the precipitation of cathodic reaction products while blocking anodic dissolution. These are generally weak acid and strong base salts such as borates, silicates, phosphates, polyphosphates, and zinc salts [21, 32, 39].

1.6.3.2.2.6. Corrosive Agent Removal Inhibition:

Only applicable in closed systems. It is particularly practiced in the closed hot water circuits of thermal power plants. A small amount of sodium sulfite (Na_2SO_3) or hydrazine (N_2H_4) added to previously degassed and deionized water removes the last traces of oxygen and thus eliminates corrosion [32].

1.6.3.4. Application of corrosion inhibitors:

Corrosion inhibitors can be distinguished for use in aqueous, organic, or gaseous media. Those used in aqueous media are selected based on the pH of the medium. Inhibitors for acidic media are used, among other things, to prevent chemical attack on metals during pickling. In the petroleum industry, they are added to drilling fluids. Inhibitors for neutral media are primarily used to protect cooling water circuits. In organic media, corrosion inhibitors are used in engine lubricants and gasoline. These fluids often contain traces of water and ionic species that can cause corrosion. Inhibitors are also used in paints (inorganic pigments or tannins). Finally, gas-phase inhibitors are generally used for temporary protection of various metal objects during transport and storage. These are most often organic compounds with high vapor pressure. These compounds adsorb onto the metal surface and protect it against atmospheric corrosion [15].

1.7. Experimental methods used to study corrosion [40]:

1.7.1. Gravimetric test:

This method has the advantage of being simple to implement and not requiring extensive equipment, but does not allow for an understanding of the mechanisms involved during

corrosion. Its principle is based on measuring the weight loss M (mg.cm-2.h-1) experienced by a sample with a surface area S during immersion time t in a corrosive solution maintained at a constant temperature.

The corrosion rate was determined after 24 hours of immersion at a temperature of 25°C. It is calculated using the following formula:

M (1) M = M1 – M2 (2)

M represents the difference between the initial mass M1 and the final mass M2 after a time t equal to 24 hours. S is the surface area of the metal exposed to the test solution. This corrosion rate value is the average of two tests carried out under the same conditions for each concentration.

The inhibitory efficiency value is given by the following formula:

EI % 100 (3)

Where , represent the corrosion rates in the absence and presence of the inhibitor, respectively.

1.7.2. Linear Polarization Resistance (LPR):

Principle:

Applying a small potential variation around the corrosion potential (±10–20 mV) to measure the current density.

Obtained parameters:

Polarization resistance (Rp), this parameter is inversely proportional to the corrosion rate.

Advantages:

- ✓ Fast.
- ✓ Non-destructive test.
- ✓ Can be used in situ.

Limitations:

- ✓ This technique requires a well-defined electrolyte solution.
- ✓ It is not always suitable for thick passive layers.

1.7.3. Potentiodynamic Polarization:

Principle:

In this technique, we exerted a wide potential range (anodic and cathodic) to plot the current-potential curve.

Obtained parameters:

- ✓ Corrosion potential (Ecorr).
- ✓ Corrosion current (Icorr).

- ✓ Passive behavior.
- ✓ Activation zones.
- ✓ Transpassivation.

Advantages:

- ✓ Mechanistic study.
- ✓ Characterization of corrosion modes can be performed with this technique.

Disadvantages:

- ✓ It is a destructive method.
- ✓ The test cannot be repeated frequently on the same sample.

1.7.4. Electrochemical Impedance Spectroscopy (EIS):

Principle:

Application of a low-amplitude alternating signal over a wide frequency range.

Obtained results:

Nyquist or Bode plots.

Extracted information:

- ✓ Corrosion resistance.
- ✓ Double-layer capacitance.
- ✓ Behavior of the protective film or passive layer.

Advantages:

- ✓ Highly sensitive method.
- ✓ Non-destructive test.
- ✓ Applicable in situ.

Applications:

- ✓ Coating monitoring.
- ✓ Assessing the corrosion inhibition.
- ✓ Long-term degradation detection.

1.7.5. Electrochemical Noise (EN):

Principle:

Measurement of spontaneous current and potential fluctuations between two identical electrodes.

Use:

Early detection of localized corrosion (pitting, stress cracking).

Advantages:

- ✓ Non-invasive method.

- ✓ Applicable to complex systems.

Limitations:

More complex data analysis; parasitic noise.

1.8. Thiophene and its derivatives as considerable corrosion inhibitors:

Five-membered heterocycles represent an important class of organic compounds due to their potential properties and applications [41]. Among these compounds, the family of thiophene derivatives is distinguished [42]. In the five-membered ring, the sulfur atom acts as an electron-donating heteroatom, contributing two electrons to the aromatic sextet; thiophene is therefore considered an electron-rich heterocycle.

The literature is indeed abundant with documents concerning the synthesis of thiophene and its derivatives, given their importance in biology [43], chemistry [44], industry [45], and medicine [46]. In addition, these compounds have proven to be excellent corrosion inhibitors for various metals and alloys.

In a study, the inhibitory effectiveness of thiophene-derived Schiff bases on the corrosion of mild steel X52 in 1 M hydrochloric acid and 1 M sulfuric acid has studied using electrochemical impedance spectroscopy measurements and surface analysis by X-ray photoelectron spectroscopy, it was reported that the presence of the Schiff base (L) behaves as a mixed-type inhibitor by inhibiting both anodic metal dissolution and the cathodic hydrogen evolution reaction. Besides, the interaction between the surface and the molecule can occur in both physical and chemical adsorption [47].

Other research examined the protection of copper against corrosion using 3-thiophenemalonic acid. The experimental data showed that the organic compound was chemically adsorbed onto the copper surface and that the inhibition mechanism was both anodic and cathodic. Khaled and collaborators have investigated the inhibitory effect of 2-thiophenecarboxylic acid methyl ester on iron corrosion in a 1M HCl solution. It was observed that the molecules under probe could act as excellent cathodic inhibitors [48].

A scientific contribution assessed the corrosion inhibitory performance of certain thiophene derivatives of the carbon steel surface in an acidic medium. The results show that the inhibition efficiency increases with increasing inhibitor concentration and temperature. They also observed that the adsorption of thiophene derivatives on the carbon steel surface obeys the Langmuir adsorption isotherm [49].

Other scientific reports demonstrated that the presence of small amounts of 2-(thiophen-3-yl)ethanamine and 2-(thiophen-2-yl)ethanamine significantly reduces the corrosion process of steel in sulfuric acid aggressive media [50,51]. Indeed, the inhibitory effect of 2-thiophene carboxaldehyde on zinc corrosion in 1M H_3PO_4 medium was studied. However, the results obtained revealed that carboxaldehyde is an effective corrosion inhibitor for zinc in H_3PO_4 solutions [52].

1.9. Conclusion:

Corrosion is a natural phenomenon that causes component degradation and failure. Although general or uniform corrosion damage results in maximum destruction of the metal component, it is easier to prevent. However, other types of corrosion, such as intergranular corrosion or stress corrosion, are highly destructive to engineering components. All these types of corrosion have an impact on the environment, the economy, and human life. The results of various studies have led to the conclusion that timely protective measures can resist corrosion.

Chapter 2: Quantum computational methods

2.1. Introduction:

The physical and chemical properties of matter in its atomic, liquid, and solid forms and their understanding can be described through the behavior of their constituents, namely the electron and the nucleus, and their interactions. The interactions among a large number of electrons give rise to the properties of solids.

The calculation of the electronic structure of molecules and solids is a field that emerged during the last century and has experienced remarkable growth over the past forty years, thanks to advances in computing and the increasing power of computers.

For calculating the electronic, structural, and mechanical properties, among others, of the most complex systems, ab-initio methods have become fundamental tools. These models are based on quantum mechanics, more specifically on the many-body Schrödinger equation.

However, since the number of interacting particles is usually enormous, solving the Schrödinger equation becomes impossible. Therefore, alternative approaches have been developed to overcome this difficulty. One such approach is Density Functional Theory (DFT).

The second chapter presents the importance of quantum chemistry, the Schrödinger equation and its resolution, and the various approximations and methods used for quantum computing. The descriptors of global reactivity and local reactivity are then detailed. This chapter concludes with a brief description of the computing software used in this local study.

2.2. The significance of quantum chemistry:

Quantum chemistry is a branch of chemistry that applies the principles of quantum mechanics, consisting of the Schrödinger equation, to study and understand the properties and behavior of chemical systems. It plays a crucial role in understanding chemical reactions, molecular structure, and the properties of materials. Here are some of the main advantages of quantum chemistry [53]:

1. Understanding chemical reactions: Quantum chemistry makes it possible to predict and explain reaction mechanisms, reaction rates, reaction products, and activation energies. This allows chemists to design more efficient chemical reactions and develop new catalysts.

2. Prediction of Molecular Structure: Quantum chemistry can determine the three-dimensional structure of molecules, including bond lengths, bond angles, and intermolecular interactions. This helps understand the chemical and physical properties of molecules, such as polarity, solubility, and reactivity.

3. Study of Material Properties: Quantum chemistry is used to study the properties of materials, including electrical conductivity, thermal conductivity, adsorption capacity, mechanical strength, and more. This allows the design of new materials with specific properties for applications such as electronics, batteries, catalysts, magnetic materials, and more.

4. Modeling Complex Chemical Processes: Quantum chemistry can model complex chemical systems such as enzymatic reactions, gas-phase reactions, and interactions between molecules under real-world conditions. This allows for a better understanding of complex chemical processes and the optimization of experimental conditions.

5. Drug Design: Quantum chemistry plays an important role in drug design by predicting the biological activity of chemical compounds, understanding their interaction with target proteins, and modeling their stability and pharmacokinetics. This facilitates the development of more effective and safer drugs. In summary, quantum chemistry offers a powerful tool for understanding and predicting the behavior of chemical systems. It enables the improvement of chemical processes, the design of new materials, and the development of more effective drugs. Its use continues to advance and have a significant impact on many areas of chemistry and materials science.

2.3. Schrödinger Equation:

Let us consider a system composed of N atoms and N electrons. In order to obtain interesting quantities such as the energy E or the wave function, which is a function of

the coordinates of the nuclei and electrons and contains all the information of the system, we must solve the time-independent Schrödinger equation, which was established by Erwin Schrödinger in 1925 [54]. It is written as follows:

$$\boldsymbol{H|\psi>=E|\psi>} \qquad (2.1)$$

Where H is the non-relativistic, non-magnetic Hamiltonian, defined as follows:

$$\mathbf{H = T_e + T_n + V_{ee} + V_{ne} + V_{nn}} \qquad (2.2)$$

Such as:

$T_e = -\sum_i^N \frac{h^2}{2m} \nabla_i^2$ *:* is the kinetic energy of the electrons.

$T_n = -\sum_A^{N_\alpha} \frac{h^2}{2M_A} \nabla_A^2$: is the kinetic energy of atoms.

$v_{ee} = \frac{1}{2} \sum_i^N \sum_{j \neq i}^N \frac{e^2}{|\vec{r_i} - \vec{r_j}|}$: is the electron-electron interaction potential.

$v_{ne} = -\sum_i^N \sum_A^{N_\alpha} \frac{z_A e^2}{\vec{r_i} - \overrightarrow{R_A}}$: is the nucleus-electron interaction potential.

$v_{nn} = \frac{1}{2} \sum_A^{N_\alpha} \sum_{B \neq A}^{N\alpha} \frac{z_A z_B e^2}{|\overrightarrow{R_A} - \overrightarrow{R_B}|}$: is the nucleus-nucleus interaction potential.

We can write the Hamiltonian H in the form:

$$\mathbf{H}= -\sum_i^N \frac{h^2}{2m} \nabla_i^2 - \sum_A^{N_\alpha} \frac{h^2}{2M_A} \nabla_A^2 + \frac{1}{2} \sum_i^N \sum_{j \neq i}^N \frac{e^2}{|\vec{r_i} - \vec{r_j}|} - \sum_i^N \sum_A^{N_\alpha} \frac{z_A e^2}{\vec{r_i} - \overrightarrow{R_A}} + \frac{1}{2} \sum_A^{N_\alpha} \sum_{B \neq A}^{N\alpha} \frac{z_A z_B e^2}{|\overrightarrow{R_A} - \overrightarrow{R_B}|} \qquad (2.3)$$

Where M, m, $\vec{r_i}$ and $\overrightarrow{R_A}$ denote respectively the mass of the nucleus, the mass of the electron i, the electronic and nuclear position vectors used to locate each of the electrons in the system and each of its nuclei A , centered on its atomic sites. The

indices i= (1,……, N) and A = (1,….., N) are thus adopted in order to distinguish electronic quantities from nuclear quantities.

The Schrödinger equation can therefore be represented in the form:

$$(Te + Tn + Vee + Vne + Vnn)\ \psi\ (r1, r2,\ldots\ldots R1,R2,\ldots.) = E\ \psi\ (r1, r2,\ldots..R1, R2,\ldots\ldots), \quad (2.4)$$

In solid-state physics, the number of interacting particles is of the order of Avogadro's number$\approx 10^{23}$. This requires a solution to a system of Schrödinger equations containing a number of simultaneous differential equations of the order of 10^{23}. Since this system of equations is difficult to solve, it is important to ensure that the equations are given even in cases of interactions involving a small number of particles. Therefore, the many approaches to solving this equation rely on a few fundamental approximations. We begin with the first approximation, the Born-Oppenheimer approximation.

2.4. Born-Oppenheimer approximation:

The first approximation was developed jointly by Born and Oppenheimer in 1927 [55]. It consists of decoupling the motion of nuclei from that of electrons. Its justification lies in the fact that nuclei are much heavier than electrons (the mass of a proton or neutron is approximately 1836 times as large as the mass of an electron). Atoms are considered to be much slower (because they are larger) than electrons. Electronic motion can thus be separated from that of nuclei: electrons then move on a potential energy surface in the field of nuclei. In other words, nuclei appear motionless to electrons. If nuclei are motionless, their kinetic energies are zero, and the interaction between nuclei becomes constant. The wave function can be written as the product of an electronic wave function and a nuclear wave function according to

$$\boldsymbol{\psi}(\vec{\boldsymbol{r}}, \vec{\boldsymbol{R}}) = \boldsymbol{\psi_n}(\vec{\boldsymbol{R}})\boldsymbol{\psi}(\vec{\boldsymbol{r}}, \vec{\boldsymbol{R}}), \quad (2.5)$$

The Hamiltonian can thus be defined as:

$$\mathbf{H= H_e+ H_n}\ , \quad (2.6)$$

Where He and Hn denote the electronic and nuclear Hamiltonians, respectively, subsequently the electronic Schrödinger equation is written:

$$\boldsymbol{He} = -\sum_i^N \frac{h^2}{2m}\nabla_i^2 - \sum_i^N \sum_A^{N_\alpha} \frac{z_A e^2}{|\vec{r_i}-\vec{R_A}|} + \frac{1}{2}\sum_i^N \sum_{j\neq i}^N \frac{e^2}{|\vec{r_i}-\vec{r_j}|}, \quad (2.7)$$

or else:

$$\boldsymbol{He} = \sum_i^N h_{i+\frac{1}{2}} \sum_i^N \sum_{j\neq i}^N \frac{e^2}{|\vec{r_j}-\vec{r_j}|}, \quad (2.8)$$

Where hi is the one-electronic Hamiltonian.

The electronic Schrödinger equation can then be written as follows:

$$\boldsymbol{H_e\psi_e = E_e\psi_e}, \quad (2.9)$$

The Born-Oppenheimer approximation is called adiabatic because it separates the electronic problem from the lattice vibration problem. This approximation significantly reduces the degree of complexity. However, since the new wave function of the system depends on N bodies, other additional approximations are required to effectively solve this equation.

2.5. Self-consistent field approximation:

2.5.1. Hartree approximation:

This approximation was first introduced by Douglas Hartree in 1928 [56]. Since Equation 1.9 is a many-body problem (due to the electron-electron interaction term), it cannot be solved exactly (except for cases involving a single electron The treatment consists of reducing the many-body problem to a single-particle problem, which allows for the consideration of approximate wave functions. For this, the simplest approximation consists of considering the electrons as independent, in which each electron moves in a mean field created by the nuclei and the other electrons, so their motion is not correlated. Thus, if we consider two electrons 1 and 2, the probability of the presence of the electron with coordinates r1 in orbital i is independent of that of the electron with coordinates r2 as exhibited by Figure 1-1.

Figure 2.1: Electron-electron repulsions.

Hartree's potential is written:

$$\boldsymbol{v^H = \int dr^3 \frac{\rho(r')}{|r - r'|}}$$

Where $\boldsymbol{v^H}$ is the Hartree potential for the i[th] electron, which replaces the electrostatic electron-electron interaction with all other electrons. The electron density in Equation 1.10 is given by:

$$\boldsymbol{\rho_i = \sum_{j(j\neq i)}^{N} \left|\phi_j(\vec{r})\right|^2} \qquad (2.10)$$

The Hamiltonian of such a system is written:

$$\boldsymbol{He = \sum_i^N h_i,} \qquad (2.11)$$

Where h_i is the one-electronic Hamiltonian defined as:

$$\boldsymbol{h_i = -\frac{h^2}{2m}\nabla_i^2 + v_{ext} + V_i^H,} \qquad (2.12)$$

$\boldsymbol{-\frac{h^2}{2m}\nabla_i^2}$: represents kinetic energy of electron i .- [1]Electrons are considered to be independent particles (independent particle approximation), and each electron in the system moves in the mean field created by the other electrons.

$\boldsymbol{v_{ext}}$: represents both the potential due to the nuclei.

$\boldsymbol{V_i^H}$: is the Hartree potential for the ith electron.

Furthermore, the total wave function is written as

$$\boldsymbol{\psi^{HP}} = (\overrightarrow{\boldsymbol{r_1}}, \overrightarrow{\boldsymbol{r_2}}, \dots, \overrightarrow{\boldsymbol{r_N}}) = \boldsymbol{\phi_i}(\overrightarrow{\boldsymbol{r_1}}), \boldsymbol{\phi_j}(\overrightarrow{\boldsymbol{r_2}}), \dots, \boldsymbol{\phi_i}(\boldsymbol{r_1}), \qquad (2.13)$$

This function is a product of single-electron spin-orbitals. It is called the Hartree Product (HP).

The hi operator has a set of eigenvalues/eigenfunctions that turn out to be spin-orbitals:

$$\boldsymbol{h\phi i}(\overrightarrow{\boldsymbol{r_i}}) = \boldsymbol{\varepsilon_i \phi_j}(\overrightarrow{\boldsymbol{r_i}}), \qquad (2.14)$$

Where $\boldsymbol{\varepsilon_i}$: is the energy associated with the presence of an electron in the orbital spin.

The Hartree potential, given by Equation 1.10, which determines the single-electron wave functions, is expressed in terms of these same wave functions according to Equation 1.11.This is why this approach is called the self-consistent field approximation.

The main flaw in the Hartree method is that it does not take into account the Pauli principle; the HP wave function is not antisymmetric with respect to the exchange of coordinates between two electrons. This method treats electrons as discernible particles and completely neglects electron correlation and exchange effects. The Hartree-Fock method is a significant refinement of the Hartree method, in which the Hartree product is replaced by a wave function given by a Slater determinant, which satisfies the condition of antisymmetry and allows the introduction of electronic exchange effects.

2.5.2. Hartree-Fock approximation:

The shape of the multi-electron wave function, which correctly describes the behavior of electrons, can be determined from considerations that take into account electron physics:

- Electrons are indistinguishable particles; electronic correlation must not be neglected.

- Electrons are fermions characterized by spatial coordinates and spin coordinates (intrinsic angular momentum).

The wave function must therefore be antisymmetric, meaning that the exchange of two electrons in the wave function must result in the appearance of a negative sign.

$$\boldsymbol{\psi(x_1, x_2) = -\psi(x_2, x_1),} \tag{2.15}$$

In 1930, Fock [57] showed that the Hartree approximation does not accept this characteristic of exchange interactions, because the Hartree multi-electron wave function violates the Pauli Exclusion Principle and does not satisfy the antisymmetry condition. To correct this flaw in the Hartree approach, Fock proposed writing the multi-electron wave function as the Slater determinant of single-electron (spin orbital) wave functions that are antisymmetric with respect to electron pair exchange:

$$\psi^{HF} = (x_1, x_\Sigma, \dots, x_N) = \frac{1}{\sqrt{N!}} \begin{vmatrix} \phi_1(x_1)\phi_2(x_2)\cdots\phi_N(x_1) \\ \phi_1(x_2)\phi_2(x_2)\cdots\phi_N(x_2) \\ . \quad . \quad . \\ . \quad . \quad . \\ \phi_1(x_N)\phi_2(x_N)\cdots\phi_N(x_N) \end{vmatrix} \tag{2.16}$$

Where $\frac{\mathbf{1}}{\sqrt{\boldsymbol{N!}}}$ is the normalization constant of this wave function, $\boldsymbol{\phi i(j)}$ denotes the i[th] spin monoelectron orbital and (j) indicates the spatial and spin coordinate of electron $\boldsymbol{j}$ grouped in the variable

The orbital spins are given by the product of an orbital function $\boldsymbol{\phi i(r_j)}$ and a spin function $\boldsymbol{\alpha(\sigma_j)}$ where

$$\boldsymbol{\sigma} = \pm\frac{\mathbf{1}}{\mathbf{2}} \begin{cases} \boldsymbol{spin} & \boldsymbol{\alpha}(\uparrow) \quad \boldsymbol{\sigma} = \frac{\mathbf{1}}{\mathbf{2}} \\ \boldsymbol{spin} & \boldsymbol{\beta}(\downarrow) \quad \boldsymbol{\sigma} = -\frac{\mathbf{1}}{\mathbf{2}} \end{cases} \tag{2.17}$$

The spin functions, $\boldsymbol{\alpha}$ and $\boldsymbol{\beta}$ obey, the condition of orthonormality:

$$\boldsymbol{\langle\alpha|\alpha\rangle = \langle\beta|\beta\rangle = 1 \ and \ \langle\alpha|\beta\rangle = \langle\beta|\alpha\rangle = 0,} \tag{2.18}$$

The Slater determinant satisfies the principle of antisymmetry because it changes sign if two rows or two columns are swapped. Swapping two rows amounts to changing the space and spin coordinates of the electron pair. We therefore have the property of antisymmetry with respect to this exchange [58].

The spin $\boldsymbol{\phi_i(r_i)}$ orbitals are the solutions to the Hartree-Fock equation:

$$\boldsymbol{F\phi_i(x_i) = \varepsilon_i\phi_i(xi)}, \qquad (2.19)$$

Where F is the Hartree-Fock operator defined for an electron by

$$\boldsymbol{F = -\frac{h^z}{zm}\nabla_i^2 + v_{ext} + V^{HF}}, \qquad (2.20)$$

Where $\mathbf{V^{HF}}$ is the Hartree-Fock potential, which represents the potential applied to electron i by the other electrons. This potential is expressed using two operators, **J** and **K** [59].

$$\boldsymbol{V^{HF} = \sum_i^N J_i(x_1) - k_i(x_1)}, \qquad (2.21)$$

With:

$$\boldsymbol{j_i(x_1)|\phi_j(x_1)} >= \left(\int \boldsymbol{\phi_i^*(x_2)\frac{1}{|\vec{r_2}-\vec{r_1}|}\phi_i(x_2)\,dx_2}\right)|\boldsymbol{\phi_j(x_1)} >, \qquad (2.22)$$

Where $\boldsymbol{j_i(x_1)}|$is the Coulomb operator representing the average repulsion potential exerted by an electron located in $\boldsymbol{\phi_i}$ on electron 1.

$$\boldsymbol{ki(x_1)|\phi_i(x_1)} >= \left(\int \boldsymbol{\phi_i^*(x_2)\frac{1}{|\vec{r_2}-\vec{r_1}|}\phi_i(x_2)\,dx_2}\right)/\boldsymbol{\phi_i(x_1)} > \qquad (2.23)$$

Where $k_i(x_1)$ is the exchange operator which comes from the anti-symmetric nature of the wave function, and has no classical equivalent: the action of $\boldsymbol{k_i(x_1)}$ on $\boldsymbol{\phi_j(x_1)}$ causes the exchange of electron 1 with electron 2.

This Hartree-Fock approximation leads to good results, particularly in molecular physics. However, it always provides an upper bound on the energy. It does not take into account electronic correlation effects because it assumes that a given electron is subject to the average influence of the electrons surrounding it, that the electron is immersed in a mean field created by the other electrons [58].The treatment of extended systems such as solids remains difficult [59]. It can therefore only handle systems with few electrons, such as small molecules. The Hartree-Fock method nevertheless remains an indispensable benchmark. This is why the density functional method is often used because it considerably and surprisingly simplifies calculations.

2.6. Density Functional Theory (DFT):

Historically, the Density Functional Theory (DFT) has its origins in the model developed by Thomas and Fermi. [60,61] in the late 1920s, but 28tw as not until the mid-1960s that the contributions of Hohenberg and Kohn [62] on the one hand and Kohn and Sham [63] on the other hand made it possible to establish the theoretical formalism on which the DFT we use today is based. It states that the energy of a multi-electron system can be expressed using the electron density, which allows the latter to be used instead of the wave function in order to calculate the energy [64].

$$\boldsymbol{E = E(\rho)} \qquad (1.24)$$

The starting point of DFT is the expression for electron density. If we consider a system comprising N electrons described by the wave function, the probability of finding the electron labeled 1 in the portion of space delimited by x_1 and dx_1 is given by [65]:

$$\boldsymbol{\rho(x_1)\, d(x_1) = N \int \psi(x_1, x_2, \cdots, x_N)\psi^*(x_1, x_2, \ldots, x_N) d_{x_2} \ldots dx_{N_1}} \quad (2.25)$$

With x_1 is the spin-orbit coordinate. $\rho(r_1)$ is the density function associated with electron 1 .Integrating over the spin coordinate $\sigma_1$allows us to define the electron density

$$\boldsymbol{\rho(r_1) = \int \rho(x_1)\, d\sigma_1,} \qquad (2.26)$$

Electron density has the following properties this theory simplifies the solution of Schrödinger equation 1.1. Here, the N electrons (3N spatial coordinates) are replaced by the total electron density which depends on only three spatial variables. The principle of DFT is to reformulate a quantum many-body problem into a one-body problem (a function of spin) with the electron density as a variable Vanishes at infinity and integrates with the total number of electrons (integrating the electron density with respect to $\boldsymbol{r_1}$ (the spatial coordinate associated with electron 1) allows us to find the number of electrons):

$$\boldsymbol{\lim_{r \to -\infty} P(r) = 0} \qquad (2.27)$$

The number of electrons per unit volume in a given state is called the electron density and it is denoted $\rho(r)$:

$$\boldsymbol{\int \rho(r_1)\, dr_1 = N\ ,} \qquad (2.28)$$

Where N represents the number of electrons in the studied system.

Unlike the wave function, electron density is an observable that can be measured by neutron X-ray diffraction.

2.6.1. Hohenberg-Kohn Theorems:

Once the various quantities have been defined, it is now necessary to lay the foundations of DFT. These were first expressed in 1964 by Hohenberg and Kohn, based on their theorems based on the idea of describing the external potential V_{ext}, and through it the total energy, as a unique functional of the density $\rho(r)$,a quantity adopted as the basic variable of DFT. They are broken down into two theorems.

First Theorem: The total energy of the ground state E of a multi-electron system is a unique functional of the electron density (r) for a given external potential V_{ext}.

Hohenberg and Kohn's first theorem states that any observable of a non-degenerate stationary ground state can be calculated, exactly in theory, by means of the electron density of this ground state. Indeed, the Hamiltonian of a system depends only on the number of electrons considered and the external potential V_{ext}, which represents the interaction between the electrons and the nuclei. The energy functional is expressed as:

$$\boldsymbol{E[\rho] = T[\rho] + V_{ee}[\rho] + v_{ext}[\rho]} \qquad (2.29)$$

Or:

- $\boldsymbol{T[\rho]}$: is the kinetic energy functional.

- $\boldsymbol{V_{ee}[\rho]}$: is the interaction potential which represents the interaction between electrons and electrons.

- $\boldsymbol{v_{ext}[\rho]}$: The external potential which represents the interaction between electrons and nuclei.

Les deux premières quantités sont rassemblées en une fonctionnelle universelle FHK, indé pendante du potentiel extérieur [65] :

$$\boldsymbol{E[\rho] = F_{Hk} + \int \rho(r_1) v_{ext}(r_1)\, dr_1,} \qquad (2.30)$$

The question here is: how can we be sure that such a density is really the density of the ground state we are looking for? The answer to this question is given by the 2nd Hohenberg-Kohn theorem [58].

Second Theorem: The total energy functional of any multi-particle system has a minimum that corresponds to the ground state and the ground state particle density [66].

Hohenberg and Kohn's second theorem states that the energy of a non-degenerate ground state can be determined by the density minimizing the ground state energy. We have:

$$\boldsymbol{E_0 \leq E[\rho]} \ , \qquad (2.31)$$

Thus, to obtain the energy of the ground state, we will seek to minimize the Energy functional, and it can be calculated by applying a similar variational principle, but this time applied to the electron density:

$$\left[\frac{\boldsymbol{\delta E[\rho]}}{\boldsymbol{\delta \rho}}\right]_{\boldsymbol{P_0}} = \mathbf{0} \ , \qquad (2.32)$$

Energy minimization is achieved through the use of the Lagrange formalism, establishing a Lagrangian with the restriction of the N-representability of the density [67]:

$$\boldsymbol{L[\rho] = E[\rho] - \mu[\rho(r)\, dr - N]}, \qquad (2.33)$$

Where $\boldsymbol{\mu}$ is the unknown Lagrange multiplier. Minimizing the Lagrangian implies:

$$\frac{\boldsymbol{\delta}}{\boldsymbol{x\rho(r)}}\{\boldsymbol{E[\rho] - \mu[\rho(r)\, dr - N]}\} = \mathbf{0} \ , \qquad (2.34)$$

as the differential of a functional is expressed in the form :

$$\boldsymbol{\delta F = \int \frac{\delta F}{\delta f} \delta f(x)\, dx} \ , \qquad (2.35)$$

We can thus rewrite 1.34 as:

$$\boldsymbol{\int \left\{\frac{\delta E[\rho]}{\delta \rho(r)} - \mu\right\} \delta \rho(r)\, dr = 0} \ , \qquad (2.36)$$

This last formula is called the fundamental equation of DFT, and implies that:

$$\boldsymbol{\mu = \frac{\delta E[P]}{sin rJ} = Vext(r) + \frac{\delta F_{Hk}[\rho]}{\delta \rho(r)}}, \qquad (2.37)$$

DFT states that, if we know the form of F_{HK} $[\rho]$, it is relatively easy to determine the ground state energy in a given V_{ext} (r). The whole problem now lies in the formulation of this functional and more precisely comes from the kinetic energy term T $[\rho]$ because its expression as a function of electron density is not known. Indeed, the two Hohenberg-Kohn theorems confirm the existence of this functional, but they no longer give its form and offer no practical guide for the explicit construction of F_{HK} $[\rho]$ and its components. The only solution to this problem, established with the aim of providing the necessary foundations to effectively exploit Hohenberg and Kohn's theorems, is the formalism proposed in 1965 by Kohn and Sham [66]. This made it possible to circumvent the difficulty in determining F_{HK} exactly. The Kohn-Sham (KS) formalism was developed from the simple observation that the exact kinetic energy of a non-interacting model system is easily calculated.

2.6.2. Kohn-Sham Approach:

In 1965, Kohn and Sham [66] developed a practical method for performing this calculation approximately. The brilliant idea was to replace the system of N real interacting particles, which was difficult to study, with a real system of independent (non-interacting) particles that could be easily studied, such that in the ground state these two systems had the same density. The starting point was a reference Hamiltonian in which the electrons did not interact with each other, V_{ee} = 0. They were only subject to the external effective Kohn-Sham potential V_s (r) = V_{eff} (r). This Hamiltonian behaved in such a way that the density extracted from solving the equations associated with H was equal to the real density of the system. In this approximation, the Hamiltonian was written as follows:

$$\boldsymbol{H_{ks} = \sum_{i=1}^{N} h_i = -\sum_{i=1}^{N} \frac{h^2}{2m} \nabla_i^2 + \sum_{i=1}^{N} V_s(r)}\ , \qquad (2.38)$$

Since H_{KS} does not contain the electron-electron interaction term, its ground-state wave function ψ_{KS} is described exactly by an antisymmetric wave function with respect to the exchange, given by a Slater determinant of the monoelectron spinorbitals $\psi(r)$ called Kohn-Sham orbitals, exactly as in the HF approximation, this determinant are obtained after solving the equation:

$$\left[-\frac{h^2}{2m}\nabla^2 + v_s\right]\phi i = \varepsilon_i \phi_i \,, \qquad (2.39)$$

Solving equation 1.39 allows us to determine the value of the kinetic energy functional without interaction T_S which does not know its expression as a function of $\rho(r)$, we know on the other hand how to calculate it by reintroducing an orbital description.

$$Ts(p) = 2\sum_{i=1}^{N/2}\left\langle \phi i \left| -\frac{h^2}{2m}\nabla_i^2 \right| \phi_i \right\rangle, \qquad (2.40)$$

It should also be noted that the Kohn-Sham formalism is not solely based on the use of electron density in the strict sense, since the calculation of the $Ts(p)$ term is done from molecular orbitals. The density is given by:

$$\rho = 2\sum_{i=1}^{N/2}|\phi_i(r)|^2, \qquad (2.41)$$

For this non-interacting system, the fundamental equation of DFT (equation 1.37) becomes:

$$\mu = V_s(r) + \frac{\delta Ts[\rho]}{\delta\rho(r)} \,, \qquad (2.42)$$

We have seen that the expression for the energy of a system containing N electrons interacting with each other is given by 1.30:

$$E[\rho] = T[\rho] + \int \rho(r) V_{ext}(r)\, dr + V_{ee}[\rho] \;, \qquad (2.43)$$

With:

T [ρ]: the kinetic energy functional of the interacting system ,-

$V_{ext}[\rho]$: the external potential,-

- $V_{ee}[\rho]$: containing both the exchange-correlation functional and the Coulomb potential. The difference between the two kinetic energies 1.40 and 1.43 is denoted $\Delta T[\rho]$ After simplifications, we find that the effective potential $V_{eff}(r)$ is given by:

$$V_{eff}(r) = V_{ext}(r) + V_{xc}(r) + \int \frac{\rho(r_2)}{|\vec{r_1} - \vec{r_2}|} dr_2 \,, \qquad (2.44)$$

where $V_{ext}(r)$ is the term due to the external potential coming from the nuclei.

$$V_{ext}(r)=\frac{\delta E_{ext}[\rho(r)]}{\delta\rho(r)} = -\sum_{A}^{N\alpha} \frac{z_A e^2}{|\vec{r}-\vec{R_A}|}, \qquad (2.45)$$

where V_{XC} (r) of the exchange-correlation energy is the exchange-correlation potential defined as a functional derivative E_{XC}:

$$\boldsymbol{V_{xc}(r) = \frac{\delta E_{xc}[\rho(r)]}{\delta\rho(r)}}, \qquad (2.46)$$

We must thus resolve:

$$\boldsymbol{h_{ks}\phi_i = \varepsilon_i\phi_i} \ , \qquad (2.47)$$

where the Kohn-Sham Hamiltonian is given by:

$$\boldsymbol{h_{ks} = -\frac{h^2}{2m}\nabla_i^2 + V_{e_{ff}}(r)}, \qquad (2.48)$$

The solution is performed as follows:

-First, a set of test molecular orbitals is used to determine the density.

-This allows the calculation of the effective potential V_{eff}(r), which allows the determination of the solutions to 1.43, namely the eigenvalues $\varepsilon_i$and the eigenvectors ϕ_i. This procedure must be repeated until convergence

2.6.3. The exchange and correlation functional:

In Expression 1.44, the only unknown is the exchange-correlation potential V_{XC} (ρ). The more precise the knowledge of this potential, the more precisely the density will be known, and therefore the closer the energy will be to the exact energy. This implies that it is necessary to find an expression for the exchange-correlation functional that most closely matches the exact expression. To this end, various exchange-correlation functionals have been proposed.

2.6.4. Local Density Approximation (LDA):

The simplest is the LDA (Local Density Approximation) approach. It was proposed in the original Kohn-Sham paper in 1965 [66], which consists of considering the density as that of a homogeneous electron gas for which the electron density is constant at all points in space, the density varies slowly with position. The electron density is assumed to be locally uniform. The influence of density variations around a point r on

the exchange-correlation is neglected, and the exchange-correlation functional is written.

$$\boldsymbol{E_{xc}^{LDA}[\rho(r)] = \int \varepsilon_{xc}^{LDA}[\rho(r)]\rho(r)\, dr,} \qquad (2.49)$$

Where $\boldsymbol{\varepsilon_{xc}^{LDA}[\rho(r)]}$ is the exchange-correlation energy density (energy/particle) of a uniform electron gas of density $\boldsymbol{(r)}$, $\boldsymbol{\varepsilon_{xc}^{LDA}[\rho(r)] = \varepsilon_{xc}^{HEG}[\rho(r)]}$. The exchange and correlation potential corresponding to equation 1.46 becomes:

$$\boldsymbol{v_{xC}^{LDA}(r) = \frac{\sigma E_{xc}^{LDA}[\rho(r)]}{\delta\rho(r)} = \varepsilon_{xc}^{LDA}[\rho(r)] + \rho(r)\frac{\varepsilon_{xc}^{LDA}}{\delta\rho(r)}} \qquad (2.50)$$

The $\boldsymbol{E_{xc}^{LDA}[\rho]}$ functional can be decomposed into the exchange contribution $\boldsymbol{E_{x}^{LDA}[\rho]}$and the correlation contribution $\boldsymbol{E_{c}^{LDA}[\rho]}$ as [17]:

$$E_{xc}^{LDA}[\rho] = E_{x}^{LDA}[\rho] + E_{c}^{LDA}[\rho] \qquad (2.51)$$

The Dirac formula [27] is given The exchange energy for a homogeneous gas of electrons $E_x^{LDA}[\rho] = -C_x \int \rho^{4/3}(r)\, dr$

$$\varepsilon_x^{LDA}[\rho] = -C_x \rho^{1/3}(r)\,, \qquad (2.52)$$

With:

$$\boldsymbol{C_x = -(3\,/\,4)\sqrt[3]{3\,/\,\pi}\,,} \qquad (2.53)$$

The method $X_\alpha$proposed by Slater [28], can be considered as an LDA where the correlation energy is neglected and the exchange part is given by:

$$\boldsymbol{\varepsilon X_\alpha[\rho] = -\frac{3}{2}\alpha C_x \rho^{1/3}(r),} \qquad (2.54)$$

Where $\boldsymbol{\alpha}$ denotes a parameter that was initially taken to be equal to 1. It was subsequently evaluated for all neutral atoms by Schwartz [68]. It should also be noted that Kohn and Sham realized that the equation $\boldsymbol{X_\alpha}$ was equivalent to LDA and was identical to the expression of Dirac 1.49 if the correlation was ignored and if in addition $\alpha = 2\,/\,3$.

For the correlation part, no explicit analytical expression of this type is known. The parameters contained in this functional were determined from the interpolation of a set of correlation energy values based on quantum Monte Carlo calculations. Finally, Ceperley and Adler [69], and more recently Ortiz and Ballone [70], have numerically determined the contribution of correlations by quantum Monte Carlo simulations.

2.6.5. The Generalized Gradient Approximation (GGA):

The LDA method is local due to the consideration of a density equivalent to that of a homogeneous gas While most of the corrections that have been introduced to LDA are based on the idea of taking into account local variations in density, the electron density gradient was introduced, leading to the Generalized Gradient Approximations (GGA), which allows for the variation in density in the vicinity of each point to be taken into account and thus allows, in many cases (but not systematically), a better description of the bond and therefore provides better results on the total energies and better geometries for weak bonds [71]. The exchange and correlation energy in GGA is written as follows:

$$\boldsymbol{E_{xc}^{GGA}[\rho(r)] = \int f\left(\rho(r), \left|\nabla \rho_{(r)}\right|\right) d_r.} \qquad (2.55)$$

We introduce the improvement factor f. Where f is a function of the local density and the gradient of the local density.

Most gradient-corrected functionals are constructed as the addition of a correction to an LDA functional. The most popular exchange functional was developed by Becke in 1988 [72] and by Perdew and Wang (PW86 and PW91) [73]. For correlation, we have the functionals of Perdew [74], Lee, Yang and Parr [75], and Perdew and Wang [76]. However, it should be noted that the GGA approximation does not necessarily lead to better results than LDA; it all depends on the property being calculated and the system being treated.

2.6.6. Solving the Kohn and Sham equations:

Solving the Kohn-Sham equations 2.39 requires:

- the choice of the basis of the wave functions to project the monoelectronic Kohn-Sham states which can be taken as a linear combination of orbitals called Kohn-Sham (KS) orbitals written in the following form:

$$\boldsymbol{\psi_i(r) = \sum_{i=1}^{M} C_{i\alpha} \phi_\alpha(r)}, \qquad (2.56)$$

Where $\psi_\alpha(r)$: are the basis functions, C_i are the expansion coefficients of the wave function i, and M represents the number of basis functions.

Solving the Kohn and Sham equations boils down to determining the coefficients $C_{i\alpha}$ for occupied orbitals that minimize the total energy.

- The choice of the form of the effective potential generated by an infinite number of nuclei or ions, the external potential, which can be determined in a self-consistent manner. From a density in$\rho^{in}(r)$, we calculate V_H and V_{XC} for a chosen approximation. The eigen states will generate a charge density out $\rho^{out}_{(r)}$different from in $\rho^{in}(r)$, a new Hamiltonian matrix must be constructed, and the corresponding eigen states are calculated.

2.7. Hybrid functionals:

Hybrid functionals combine the exchange-correlation of conventional GGA methods with an exact Hartree-Fock percentage exchange. Providing a significant improvement over GGA functionals for many properties, they have become very popular and are now widely used. Among the best known are the PBE0 functional [45, 46] and the B3LYP functional [47]. Hybrid meta-GGA methods (HM-GGAs) represent a new class based on the same concept as meta-GGA functionals. The difference lies in the fact that they are derived from meta-GGA functionals rather than standard GGA functionals. Therefore, these functionals depend on the Hartree-Fock exchange, the electron density, its gradient, and the kinetic energy density. These methods represent an improvement over previous formalisms, particularly in determining energy barriers and atomization energies. Examples include the meta-GGA hybrid functionals M06 [48, 49] and M0-62X [50] used in my work. Recently, a new range of hybrid functionals characterized by an exact Hartree-Fock exchange percentage that varies with the intramolecular distance has emerged to address, in particular, the long-range exchange potential (Range separated hybrids functionals)

that classical hybrid functionals cannot adequately address. Examples of these so-called long-range functionals include the CAM-B3LYP (Coulomb Attenuated Model-B3LYP) functional [51] and the LC-PBE (Long-range-Corrected-PBE) functional [52].

2.8. Solvation Method [63]:

We have seen how to obtain the electronic energy, electron density, and energy for an isolated molecule. The ability to integrate solvent effects into the calculation of various properties of chemical systems remains a challenge in quantum chemistry, as it involves the intervention of statistical mechanics and therefore adds higher-order difficulties. Given that the majority of chemical and biological reactions take place in solution, theoretical chemists prefer to use models that account for solvent effects. Two main classes of solvation models are distinguished: • Discrete models, in which the solvent molecules are explicitly treated in the calculation. They are suitable for accounting for short-range solute-solvent interactions. The major drawback of this technique is the considerable increase in the size of the system to be modeled. • Continuum models, in which the solvent effects are simulated by a dielectric. They are suitable for reproducing solute-solvent interactions by simulating an electric field created by the solvent. This technique is considered in this work.

2.8.1. The Polarizable Continuum Model (PCM) [63]:

The Polarizable Continuum Model (PCM) is a good approach for representing solvation effects, due to the reduced computational time required to simulate a molecule in solution. Another advantage is that the continuum model is a systematic approach that eliminates the need to construct solvation shells for each system studied. In the continuum model, the system considered is an infinitely dilute solution at equilibrium, represented by the dielectric constant of the real solvent. Using this model, which is based on the principle of the self-consistent reaction field (SCRF), all average interactions between the solute and the solvent at thermal equilibrium are calculated. This approximation is only valid if no specific interactions exist between the solute and the solvent. To calculate the solute-solvent interaction energy, the first step is to define the solute-solvent boundary obtained by forming a cavity that encloses the solute within the dielectric medium and is inaccessible to the solvent. This cavity is constructed using spheres centered on each atom so as to respect the shape of the solute; it has a dielectric constant equal to 1 to simulate a vacuum. The

external dielectric medium has the dielectric constant of the solvent in question εs. In a second step, the solute is placed in the cavity and interacts with the continuum. This interaction takes place through the charge distribution of the solute, which polarizes the surface of the continuum cavity. Charges appear at the solute-continuum interface and induce a reaction potential that modifies the electron density of the solute. The continuum must then adapt to a new change in the charge distribution that appears at the solute-continuum interface, and so on until electrostatic convergence is achieved between the solute-specific charge distribution and that of the cavity surface. The total solute-solvent interaction energy is given by: The dispersion and repulsion terms (ΔEdis /(ΔErep) are related to the solute-solvent interactions at the cavity interface. The total electronic energy of the solvated molecule is the sum of the solute's electronic energy Eélec calculated by the DFT method in the absence of the solvent and the interaction energy (ΔEdinter between the solute and the solvent). The PCM model used in this work is the Cancès-Tomasi integral equation formalism implemented in the Gaussian software.

2.9. Global and local reactivity descriptors:

Global and local reactivity descriptors are tools derived from density functional theory (DFT) used in theoretical and computational chemistry to predict the chemical reactivity of a molecule or a particular site within that molecule. They allow us to understand where and how a molecule is likely to react [69].

2.9.1. Global reactivity descriptors:

They characterize the reactivity of the entire molecule.

- **HOMO and LUMO energy:**

- The Highest Occupied Molecular Orbital HOMO gives an idea of the molecule's ability to donate electrons.

- The Lowest Unoccupied Molecular Orbital LUMO gives an idea of its ability to accept electrons.

- The HOMO-LUMO gap provides an indication of chemical stability and reactivity: a small gap generally indicates a more reactive molecule.

- **Ionization potential:**

The energy required to remove an electron from a neutral molecule.

$$I = -E_{MOMO} \qquad (2.57)$$

- **Electron affinity:**

The energy released or consumed when a molecule captures an electron.

$$A = -E_{LUMO} \qquad (2.58)$$

- **Electronegativity:**

This quantum parameter measures a system's tendency to attract electrons.

$$X = \frac{I + A}{2}$$

- **Chemical Hardness and softness:**

Measures a system's resistance to changing its electron density.

$$\eta = \frac{I-A}{2} \qquad (2.59)$$

$$\sigma = \frac{1}{\eta} \qquad (2.60)$$

- **The fraction of electrons transferred**

The fraction of electrons transferred from the corrosion inhibitor to the electron deficient metal is defined using the equations below:

$$\Delta N = \frac{X_{Fe}-X_{in}}{2(\eta_{Fe}+\eta_{in})} \qquad (2.61)$$

2.9.2. Local reactivity descriptors

These identify specific reactive sites in a molecule.

- **Fukui functions**

Indicates the local reactivity of an atom during a nucleophilic or electrophilic attack:

•For a nucleophilic attack (addition of electrons):

$$F^+ = q^A_{N+1} - q^A_N \qquad (2.62)$$

•For an electrophilic attack (withdrawal of electrons):

$$F^- = q^A_N - q^A_{N-1} \qquad (2.63)$$

2.10. Molecular dynamics (MD) simulation:

Molecular dynamics (MD) simulation is a widely used computational method for studying interactions between molecules at the atomic level, particularly in the field of corrosion inhibitors. Here is a structured overview of how this approach can be applied to study a corrosion inhibitor.

Molecular dynamics simulation allows:

- To observe in detail the adsorption of the inhibitor on the metal surface.

- To predict the physicochemical properties (adsorption, diffusion, interaction energy).
- To analyze the stability of the inhibitor layer.
- To study the effect of different parameters (pH, temperature, concentration, metal type).

2.11. Calculation programs used in this study:

2.11.1. Gaussian:

Gaussian is a very powerful computational chemistry software program, originally created by John Pople and released in 1970. This quantum chemistry program gets its name from Pople's use of Gaussian orbitals to speed up calculations compared to software using Slater orbitals. Gaussian can predict energies, molecular structures, vibrational frequencies, and many molecular properties from these basic types of calculations [77].

2.11.2. HyperChem:

HyperChem is chemical molecular modeling software developed by Hypercube Inc. It works by combining 3D visualization and animation with quantum chemistry calculations, molecular mechanics, and dynamics. It is easy and flexible. HyperChem Release 8.0 integrates even more powerful computational chemistry tools than ever before, as well as support for several third-party applications. Its drawing and rendering capabilities and ease of use are industry standards [78].

2.11.3. Materials Studio:

Materials Studio is a molecular modeling and materials simulation software developed by BIOVIA Accelrys. It is widely used in the fields of chemistry, materials, physics, and nanotechnology to model, simulate, visualize, and analyze molecular and crystalline structures [79].

2.11.3.1. Materials Studio Key Features:

- Molecular and crystal modeling.
- Construction of molecular structures, polymers, crystals, and surfaces.
- Interactive 2D/3D visualization.
- Quantum and atomistic simulation.
- Materials properties analysis including electronic, mechanical, and thermal properties.
- Adsorption, diffusion, chemical reactivity.

- Simulated IR, Raman, and NMR spectroscopy.
- Simulation of amorphous materials.
- Design of new materials (semiconductors, catalysts, composites.
- Studies of surfaces and interfaces.
- Nanotechnology research.

Chapter 3: Results and discussion

3.1. Introduction:

The final chapter of our study focuses on correlating previously reported experimental results on corrosion, with the aim of better understanding the behavior of corrosion inhibitors at the molecular level. This chapter adopts a comprehensive approach. First, we present the selected experimental study, highlighting some essential information such as the materials used, experimental conditions, and results obtained. Next, we describe in detail the DFT, SAR, and MD procedures. We explain the underlying principles of these methods and their applications in our study. This section highlights the molecular and electronic aspects involved in the corrosion process and the effectiveness of the inhibitors studied. Finally, we provide an in-depth discussion of the global reactivity parameters. We also analyze the Mulliken charges to better understand the electronic distribution of the molecules under probe. In addition, we examine SAR indices and to assess the relationship between the molecular structure of inhibitors and their anticorrosion activity. MD simulation has been performed to give more insights about the interactions between the examined compounds and the carbon steel and to reveal the adsorption type of each corrosion inhibitor. The objective of this discussion is to clarify the role of each studied molecule and to identify the key factors contributing to their effectiveness as corrosion inhibitors.

3.2. Experimental background:

A.S. Fouda and co-workers synthesized two thiophene derivatives, namely 2-thiophene carboxylic acid (TC1) and 2-thiophene carboxylic acid hydrazide (TC2) as shown in Figure 3.1 [8]:

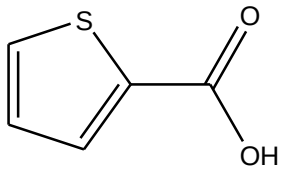

2-thiophene carboxylic acid

TC1

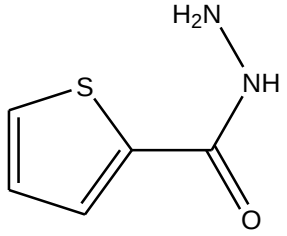

2-thiophene carboxylic acid hydrazide

TC2

Figure 3.1: Molecular structures of the tested derivatives.

Their anticorrosion properties for carbon steel in a 1 M HCl solution were studied by electrochemical impedance spectroscopy and potentiodynamique polarization at 293 K. The reported results are shown in Table 3.1.

Table 3.1: Corrosion potential (E_{corr}), corrosion current density (i_{corr}), Tafel slopes (β_c,β_a), and inhibition efficacy (IE) in 1M HCl at 298K for tested molecules

Medium	Concentration (mol/L)	E_{corr} (Mv/Ag/AgCl)	i_{corr} ($\mu A/cm^2$)	β_c (mV/dec)	β_a (mV/dec)	IE (%)
1 M HCl		453	972	200	129	
TC1	1×10^{-5}	547	190	102	884	80.5
	3×10^{-5}	584	141	89	617	85.5
	5×10^{-5}	542	121	101	152	87.6
	7×10^{-5}	536	117	128	123	88.0
	9×10^{-5}	538	108	114	136	88.9
	11×10^{-5}	531	86.1	105	145	91.1
TC2	1×10^{-5}	538	99.2	109	130	89.8
	3×10^{-5}	506	90.4	122	104	90.7
	5×10^{-5}	473	55.0	130	85	94.3
	7×10^{-5}	506	51.7	119	96	94.7
	9×10^{-5}	503	46.3	116	94	95.2
	11×10^{-5}	382	22.1	124	33	99.7

From the previous results, it is found that the corrosion inhibition efficiency of TC2 molecule is higher than that of TC1 molecule. We make a theoretical calculation to understand the close relationship between the anticorrosive efficiency of the studied thiophene derivatives and their electronic properties at the molecular scale.

3.3. Calculation details:

3.3.1. Calculation of global reactivity indices:

In this theoretical study, the Gaussian 03 program was used to perform the necessary aqueous-phase calculations of overall reactivity parameters. The GaussView 6.0 program was used to process the Molecular Model files of the compounds studied and run the quantum computations. The geometric optimization of the molecular structures of the corrosion inhibitors studied was based on density functional theory (DFT), combined with the very popular hybrid Becke, three-parameter, Lee-Yang-Par B3LYP functional. To ensure the accuracy of the calculations, the 6-31G basis set was used, recognized for its high accuracy in determining geometries and electronic properties for a wide range of organic compounds [80].

Since electrochemical corrosion occurs in a liquid phase, it is appropriate to consider the effect of the solvent in the calculations. For this purpose, the coherent reaction field theory (SCRF) with Tomasi polarized continuum model (PCM) was used to perform the solution calculations. This theoretical approach models the solvent molecules as a field of uniform dielectric constant (DC = 78.5) and defines a cavity where the solute is placed as a uniform series of nested atomic spheres [81]. Log-type results are used to calculate the global reactivity indices, as mentioned in Chapter II. The obtained chk files are used to visualize the HOMO and LUMO frontier orbitals distribution within the molecules under investigation.

3.3.2. Mulliken charge analysis:

The contribution of each atom to the electron transfer between the inhibitors examined and the metal substrate during corrosion protection was estimated by analyzing the Mulliken charges; these charges are calculated at the DFT/B3LYP/6-31G level of theory.

3.3.3. SAR parameter calculations:

Structure-activity relationship (SAR) indices including polarizability, surface area, molecular volume, and Log P partition coefficient were calculated using HyperChem 8.0 software.

3.3.4. Molecular dynamic simulation:

The interaction between the studied compounds and Fe (111) surface was performed using discover module and carried out in a simulation box with periodic boundary conditions and COMPASS force field (Condensed Phase Optimized Molecular Potentials for Atomistic Simulation Studies) was used to optimize the structures of all components of the system [4]. Firstly, The Fe crystal was imported and cleaved along (111) plane and a slab of 6 Å was employed. The Fe (111) surface was relaxed by minimizing its energy using smart minimizer method, and then enlarged to a (10 × 10) supercell to provide a large surface for the interaction of the inhibitors. A vacuum slab with zero thickness was built. An amorphous cell was then constructed with the optimized configuration of the inhibitors and water. All the atoms in Fe (111) surface were kept frozen during the simulation process, only the inhibitors and water molecules were allowed to contact the aluminum surface freely. Nonbonding, van der Waals and electrostatic interactions were set as atom-based summations using the Ewald summation method with a cutoff radius, spline width, and buffer width were set as 15.5 Å, 1 Å, and 0.5 Å, respectively. The Andersen algorithm [6] was employed to control the temperature of simulation at different levels. The simulation was performed at 298 K, NVT ensemble, with time step of 1 fs and simulation time of 50 ps. The dynamic process was performed until the entire system reached equilibrium, at which both the temperature and the energy of the system were balanced.The interaction energy $E_{interaction}$ between Al surface and

inhibitor molecule and the binding energy B_{inding} was calculated using the following equations [7]:

$$E_{interaction} = E_{total} - (E_{surface} + E_{inhibitor} + E_{solution}) \quad (11)$$

$$E_{binding} = -E_{interaction} \quad (12)$$

Where the E_{total} is defined as the total energy of the entire system, $E_{surface}$ and $E_{solution}$ are defined as the total energy of iron surface and Solution respectively. the $E_{inhibitor}$ is the energy of the adsorbed inhibitor molecule on the surface.

3.4. Results and discussion:

Figure 3.2 shows the optimized molecular structures of the corrosion inhibitors studied, calculated in aqueous phase at the DFT/B3LYP/6-31G level of theory.

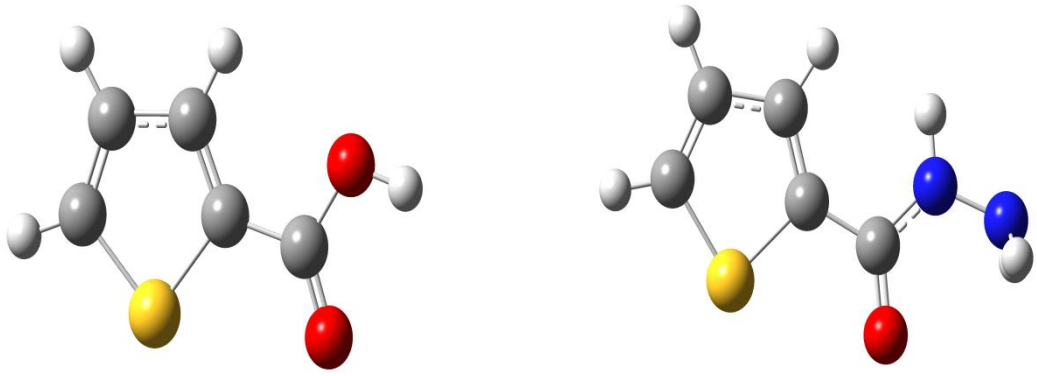

TC1 **TC2**

Figure 3.1: The optimized molecular structures of the studied corrosion inhibitors, calculated in aqueous phase at the theoretical level DFT/B3LYP/6-31G.

3.4.1. Results of global reactivity parameters:

Quantum chemical parameters such as E_{HOMO}, E_{LUMO}, energy gap ($\Delta E = E_{LUMO} - E_{HOMO}$), chemical hardness and its reciprocal, chemical softness, electronegativity, chemical potential, proton affinity, electrophilicity, and nucleophilicity are very effective and useful indices in metal corrosion studies. The global reactivity indices of the studied corrosion inhibitors were calculated in the aqueous phase and then collected in Table 3.2. In what follows, we will discuss the effect of each of the descriptors mentioned in the table on the corrosion inhibition effectiveness.

Table 3.2: Global reactivity descriptors of the studied corrosion inhibitors, calculated in the aqueous phase at the DFT/B3LYP/6-31G theoretical level.

Parameter	TC1	TC2
μ	4.2743	5.4781
E_{HOMO}	-6.9294	-6.7253

E_{LUMO}	-1.8871	-1.5536
ΔE	5.0423	5.1717
I	6.9294	6.7253
A	1.8871	1.5536
η	2.5211	2.5858
σ	0.3966	0.3867
χ	4.4083	4.1395
ω	3.8540	3.3133
ΔN	3.2671	3.6984

The concept of frontier molecular orbitals (FMOs) proposed by Fukui Kinachi is very useful for interpreting chemical reactivity. The electronic transition is attributed to the overlapping interactions between the HOMO and LUMO orbitals of the reagents studied. It has been found that the ability of a corrosion inhibitor molecule to donate an electron to the deficient metal substrate increases with increasing HOMO energy (E_{HOMO}) [82]. In general, a higher HOMO energy results in increased inhibition efficiency. The E_{HOMO} energy results presented in Table 3.2 revealed that the inhibitor TC2 has a higher E_{HOMO} energy than TC1, which is consistent with previously reported experimental inhibition efficiency results.

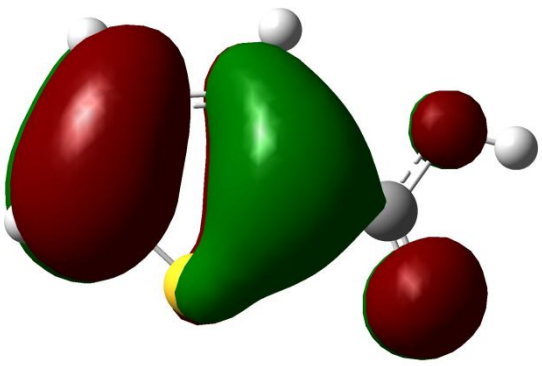

HOMO of TC1

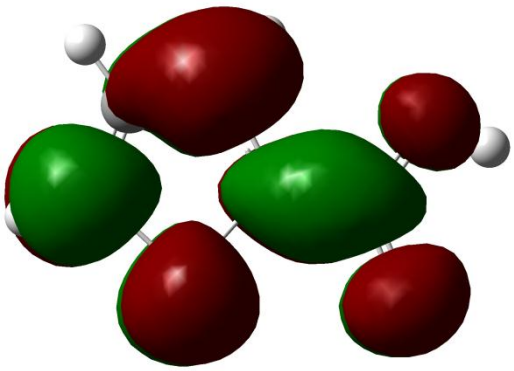

LUMO of TC1

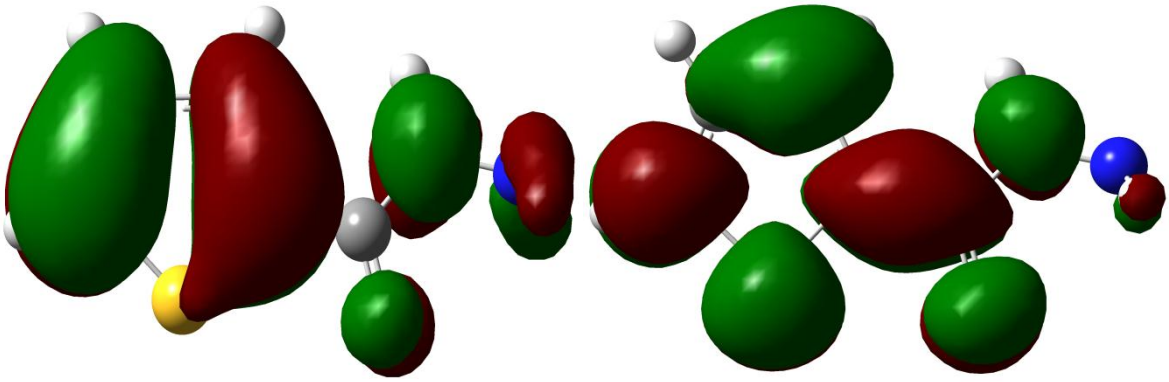

HOMO of TC2 **LUMO of TC2**

Figure 3.3: The electronic distribution of the HOMO and LUMO frontier orbitals across the molecular structures of the examined corrosion inhibitors.

The chemical reactivity of inhibitor molecules is also assessed using another important quantum descriptor: the energy gap (ΔE), which is the difference between the E_{LUMO} and E_{HOMO} values. It is expected that a chemical species with the smallest energy gap will be more reactive and will better protect the metal surface [83]. The theoretical results, presented in Table 3.2, show that the ΔE values of the corrosion inhibitors studied follow the trend: TC2 > TC1, which is in contradiction with the experimental results.

The global chemical hardness (η) and its inverse; the chemical softness (σ), are two indicators of reactivity; chemical hardness quantifies the resistance of a molecule to deformation or polarization of the electron cloud induced by a chemical reaction. Corrosion inhibitor molecules with lower chemical hardness values are more effective in protecting metals [84]. The results presented in Table 3.2 indicate that the chemical hardness of thiophene derivatives follows the trend: TC2 > TC1, which implies that the chemical softness follows the opposite trend: TC1 > TC2. These results do not validate the order of corrosion inhibitory effectiveness previously reported.

Electronegativity (χ) represents the ability of an atom in a chemical compound to attract the shared electron pair. This quantum index is useful for evaluating the chemical reactivity of corrosion inhibitors. Molecules with lower electronegativity are expected to have an excellent inhibition effect [85]. As shown in Table 3.2, the electronegativity (χ) of TC2 is lower than that of TC1, suggesting that TC2 could protect the carbon steel against corrosion better than TC1, which validates the previously reported experimental observations.

The fraction of electrons (ΔN) transferred from the corrosion inhibitor to the electron-deficient metal is an important quantum parameter that can be calculated using the Pearson equation. An inhibitor molecule can donate electrons to the metal if its parameter (ΔN) is

positive and less than 3.6. A higher value of ΔN indicates an increased tendency of the inhibitor to offer electrons to the deficient d orbital of the metal surface, leading to maximum corrosion protection [86]. The ΔN data indicate that the studied inhibitors are electron donors, with electron donation following the sequence: TC1 < TC2, which correlates well with the experimental results.

The dipole moment (μ) verifies the polarity of chemical species with covalent bonds. A chemical compound with a dipole moment value different than zero is of polar nature. The dipole moment (μ) is a beneficial reactivity parameter; an inhibitor molecule with a high dipole moment can easily adhere to the metal, forming a barrier layer capable of protecting the surface against different aggressive agents, thus increasing the inhibition efficiency [87]. The dipole moment (μ) values collected in Table 3.2 increase as follows: TC1 < TC2. This result is in excellent agreement with the previously reported experimental corrosion inhibition results.

3.4.2. Mulliken charge analysis results:

The use of Mulliken charges is a commonly used method to identify electrophilic and nucleophilic attack sites in a molecule. These charges provide a distribution of electron densities between different atoms, which helps understand the chemical reactivity of various regions of the molecule. Mulliken charges are obtained from molecular orbital coefficients and electron population densities calculated using quantum computing methods, including the Hartree-Fock method or DFT. By assigning a specific electron density to each atom, they allow us to evaluate the distribution of electrons within the molecule.

Nucleophiles are electron-rich species that attack electron-poor regions. In a molecule, nucleophilic sites are generally atoms with negative Mulliken charges or more negative charges compared to other atoms in the molecule [88]. Electrophiles are electron-poor species that attack electron-rich regions. In a molecule, electrophilic sites are generally atoms with positive Mulliken charges or less negative charges relative to other atoms in the molecule [10].

The Mulliken charge distribution across a molecule can be used to predict the potential adsorption center. For corrosion inhibitors, the greater the negative charge, the greater its electron-donating capacity. The most negatively charged regions are the most likely adsorption centers. The Mulliken charges and their numbering for each corrosion inhibitor studied are listed in Table 3.3 and Figure 3.4, respectively.

Table 3.3: The Mulliken charge values, calculated in the aqueous phase at the DFT/B3LYP/6-31G theoretical level.

TC 1		TC 2	
Atom	**Charge**	**Atom**	**Charge**
C1	-0.3623	C1	-0.4008
S2	0.4363	S2	0.4128
C3	-0.2337	C3	-0.2443
C4	0.1073	C4	0.0982
C5	0.1730	C5	0.1589
C6	0.5078	C6	0.5600
O7	-0.4959	O7	-0.5581
O8	-0.1324	N8	-0.1618
-	-	N12	0.1352

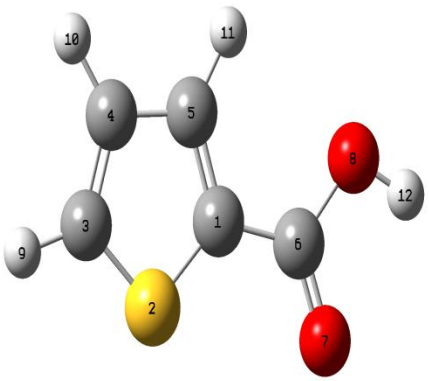

TC1

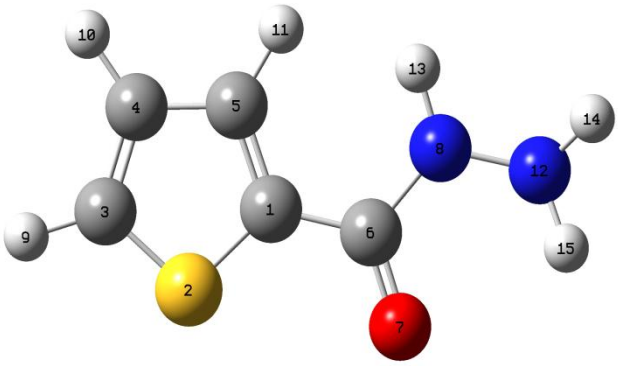

TC1

Figure 3.4: Numeration of the atoms in the studied molecules.

From the values listed in the mentioned table, it can be seen that the most favorable sites for interaction between TC1 and the metal surface are the following atoms: C3 and O8, as these atoms have a higher negative charge, suggesting that these active power plants with excess charges can act as a nucleophilic reagent. For TC2, the atoms C3 and N8 possess the highest negative charges compared to the other atoms, which indicates the high tendency of these atoms to participate in the nucleophilic attack with the electron-deficient metal.

3.4.3. SAR parameters results:

SAR calculations were performed using HyperChem software, and the obtained parameters are listed in Table 3.4.

Table 3.4: SAR parameters of the examined thiophene derivatives.

Parameter	TC1	TC2
α	12.51	14.58
LogP	-0.41	-1.29
V	381.85	438.34
S	239.38	254.79
HE	-7.56	-13.90

Polarizability (α) measures the ability of chemical species to change their electronic distribution under the influence of an electric field. An increase in polarizability increases the intrinsic molecular value, thus facilitating the adhesion of the inhibitor to the metal substrate [88]. The results in Table 3.4 show that TC2 exhibits a higher polarizability (α) than TC1, in excellent correlation with previously reported inhibition rates.

The partition coefficient (Log P) is a key indicator for assessing the anticorrosive efficacy of the tested chemical species. As the water solubility of the inhibitor decreases due to its increasing hydrophobicity, electronic transport to the metal surface becomes more difficult and slower. This reduces the adhesion of the inhibitor molecule to the metal substrate [88]. As shown in Table 3.4, the Log P decreases in the following order: TC1 > TC2, which validates the experimental results.

The hydration energy (HE) of a molecule indicates its degree of dissolution. This parameter is crucial for evaluating anticorrosive activity. An increase in hydration energy (HE) tends to improve the molecule's inhibition efficiency [88]. The data in Table 3.4 show that the hydration energy follows the order: TC2 < TC1, thus contradicting the experimental results.

The surface area (SA) is a key indicator of corrosion protection. An inhibitor with a larger specific surface area tends to adsorb more extensively on the metal surface, thus increasing its effectiveness [88]. The results in Table 3.4 demonstrate that TC2 has a larger specific surface area than TC1, resulting in a larger surface coverage and increased inhibitory efficiency, in excellent agreement with the experimental results.

The molecular volume (V) illustrates the ability of an inhibitor compound to cover a metal surface. Molecules with a flat structure and a large molecular volume have a strong tendency to cover a large metal surface, thus providing high protection performance. The inhibition efficiency therefore increases with the molecular volume [88]. A comparison of the molecular volume values of the studied structures reveals the following order: TC2 > TC1, expecting that the inhibition efficiency follows the order TC2 > TC1, which is in perfect consistency with the reported experimental data.

3.4.4. Molecular dynamics simulation outcomes:

MD simulations have been performed in order to gain a sufficient understanding of the inhibition mechanism. Figure 3.5 represents the best adsorption configuration (side and top view) of neutral thiophene based corrosion inhibitors on the carbon steel surface, respectively, the corrosion inhibitors horizontally adsorb on the iron surface with planar and flat configurations indicating better protection performance because it can cover a larger metallic surface [89].

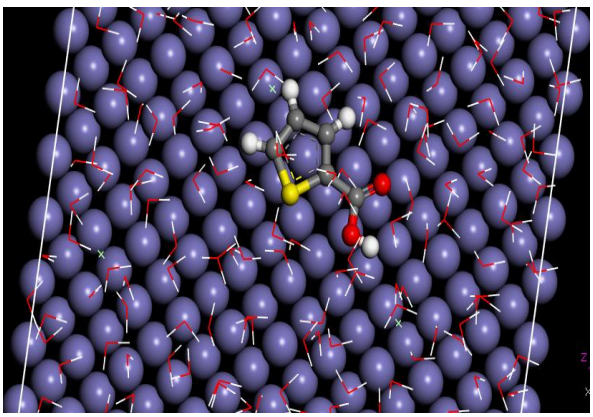

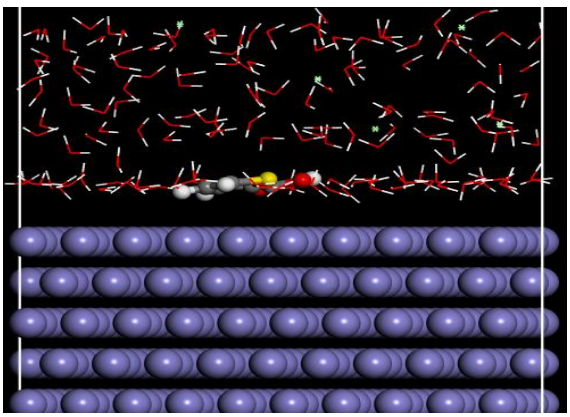

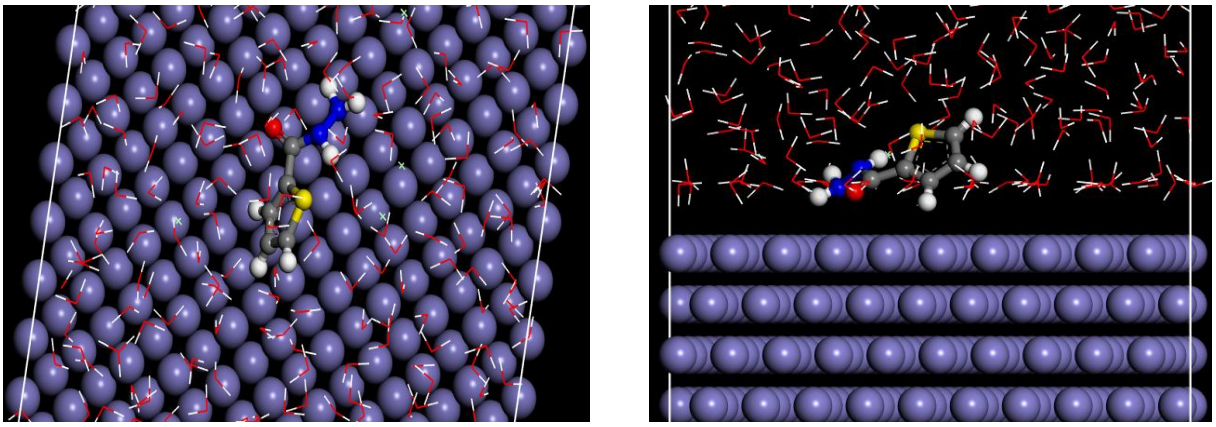

Figure 3.5: Equilibrium adsorption configurations of the studied inhibitors on Fe (1 1 0) surface obtained by molecular dynamics simulations top and side view.

The negative values of adsorption energies displayed in Table 3.5 confirmed that the adsorption of the thiophenes under investigation on metallic surface spontaneous, stable, and strong. However, the binding energy data given in Table 3.5 increased in the sequence TC1 < TC2. These theoretical outcomes are in good correlation with the tendency of the reported inhibition efficacies of earlier experimental study.

Table 3.5: The interaction energy obtained from MD simulation for adsorption of TC1 and TC2 molecules on Fe (1 1 0) surface.

System	Interaction energy (Kcal/mol)	Binding energy (Kcal/mol)
TC1+Fe+H_2O	-875.69	875.69
TC2+Fe+H_2O	-951.02	951.02

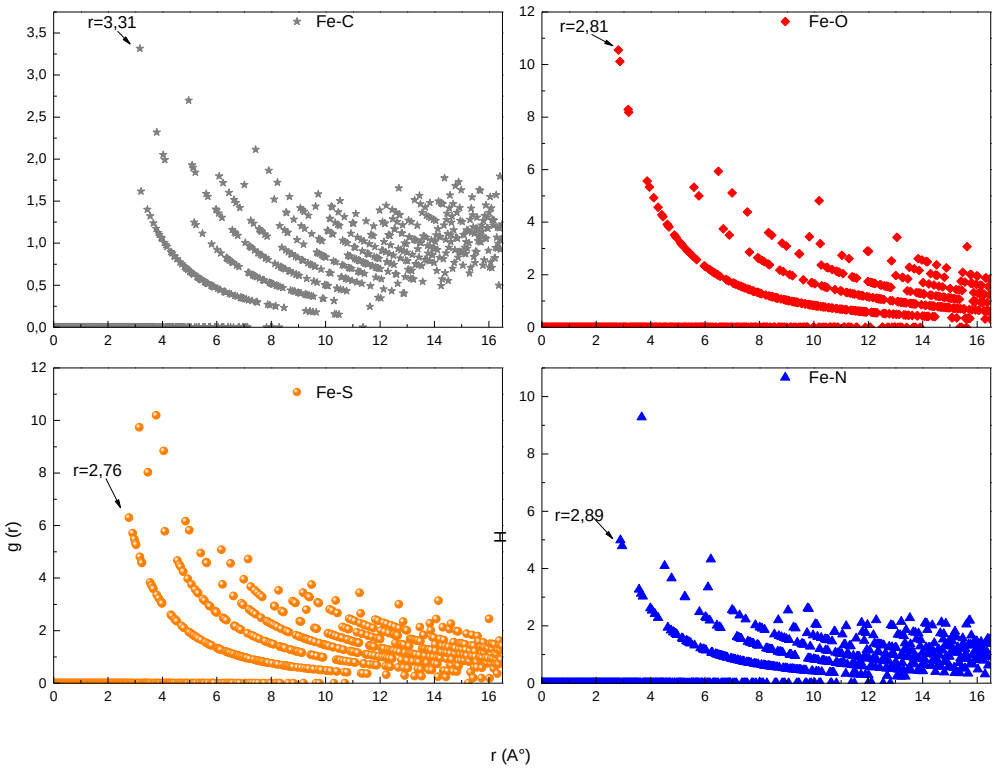

Figure 3.6: Pair correlation functions of Fe–N, Fe–C, Fe–S, and Fe–O in the examined molecules.

The analysis of pair correlation function g(r) can inform about the bond length and the interaction modes between the inhibitor molecules and the mild steel surface. Generally, the peak value of g(r) less than 3. A◦ demonstrated that a chemical bond was generated between the active centers of the inhibitor and metal atoms (chemisorption) whereas the peak value of g(r) of greater than 3.5 A◦ indicating that a Van Der Waals and/or a Coulomb type interactions (physisorption) [90]. Figure 3.6 shows that the bond lengths of Fe–N, Fe–C, Fe–S, and Fe–O are less than 3.5 A◦, which indicates that the tested inhibitors adhere to the iron surface via chemical adsorption.

General conclusion

General conclusion

In this scientific contribution, we performed aqueous DFT calculations at the DFT/B3LYP/6-31G theoretical level, structure-activity relationship calculations as well as MD simulation to correlate the anticorrosive properties of two thiophene derivatives with their electronic properties at the molecular level. The previous results discussions allow us to conclude:

- The global reactivity descriptors including dipole moment, E_{HOMO}, electronegativity, and electrophilicity are in excellent agreement with the previously reported order of corrosion inhibition efficiency.
- The Mulliken charge analysis for both inhibitors studied is convincing and presents a reactive scheme that monitors the active atomic sites responsible for electron transfer.
- The SAR parameters, including polarizability, partition coefficient, surface area, hydration energy, and volume, validate the experimental results.
- MD results confirmed the experimental outcomes earlier reported.

[1] M. I. Khan, A. Sarkar, H. K. Mehtani, P. Raut, A. Prakash, M. J. N .V. Prasad, I. Samajdar and S. Parida, Mater. Chem. Phys., 2022, 290, 126623.

[2] A. Bousskri, A. Anejjar, M. Messali, R. Salghi, O. Benali, Y. Karzazi, S. Jodeh, M. Zougagh, E. E. Ebenso and B. Hammouti, J. Molec. Liquids, 2015, 211, 1000–1008.

[3] K.F. Khaled, Electrochimica Acta, 55, 22, 2010, Pages 6523-6532.

[4] Said Abbout, Meryem Zouarhi, Driss Chebabe, Mohamed Damej, Avni Berisha, Najat Hajjaji, Heliyon,6, 2020, e03574.

[5] Ohoud S. Al-Qurashi, Nuha Wazzan, Journal of Saudi Chemical Society, 26, 2022, 101566.

[6] X.Y. Zhang, Q.X. Kang, Y. Wang, Computational and Theoretical Chemistry, 1131, 2018, 25-32.

[7] A. H. Ahmed, M. El-Sayed Sherif, S. Hany Abdo, E. S. Gad, ACS Omega, 6, 2021, 14525-14532.

[8] A. S. Fouda, A. A. Ibrahim and W. T. El-behairy, Der Pharma Chemica, 2014, 6(5):144-157.

Chapter 1

[9] Akpanyung K. V., & Loto, R. T. (2019). Pitting corrosion evaluation: a review. J. Phys.: Conf. Ser. 1378 022088, 1-15.

[10] Altenpohl, D., & Zeiger, H. (1965). Corrosion. in: aluminum. Springer. 19. https://doi.org/10.1007/978-3-662-30245- 3_17

[11] Armijo, J. S. (1968). Intergranular corrosion of nonsensitized austenitic stainless steels. Corrosion, 24(1), 24-30. https://doi.org/10.5006/0010-9312-24.1.24

[12] Berradja, A. (2019). Electrochemical Techniques for Corrosion and Tribocorrosion Monitoring: Fundamentals of Electrolytic Corrosion. Corrosion Inhibitors. doi:10.5772/intechopen.85392.

[13] Charng, T., & Lansing, F. (1982). Review of corrosion causes and corrosion control in a technical facility. Jet Propulsion Lab., Pasadena, CA (USA).

[14] Curley-Fiorino, M. E. & Schmid, G.M. (1980). The effect of the Cl− ion on the passive film on anodically polarized 304 stainless steel. Corrosion Science, 20(3), 313-329. https://doi.org/10.1016/0010-938X(80)90002-5

[15] Davis, J. R. (2001). Surface engineering for corrosion and wear resistance. ASM International, 279.

[16] Décarie, E. L., & Geider, R. J. (2017). Predictions of response to temperature are contingent on model choice and data quality. Ecol Evol, 7(23), 10467-10481.

[17] Eliaz, N. (2019). Corrosion of Metallic Biomaterials: A Review. Materials. 12(3),400-407. doi: 10.3390/ma12030407

[18] Evgueni, B., Nikolay P., & Boris S. (2004). Truncated-determinant diagrammatic monte carlo for fermions with contact interaction. Phys. Rev. 70, 15-28.

[19] Fernandes, J. S., & Montenor, F. (2015). Corrosion. Materials For Construction And Civil Engineering, 2, 679-716. doi:10.1007/978-3-319-08236-3_15

[19] Giurlani & Innocenti, M. (2018). Electroplating for decorative applications: recent trends in research and development walter. Coatings, 8, 149-260. doi:10.3390/coatings8080260

[20] Goldstein, E. M. (1960). The Corrosion and oxidation of metals: scientific principles and practical applications. J. Chem. Educ. 37, 662-672.

[21] Hoar, T. P. (1949). Bulk metallic glasses: an overview. Trans. Faraday Soc. 45, 683-692.

[22] Hoar, T. P. & Agar, J. N. (1947). Factors in throwing power illustrated by potential-current diagrams. Discuss. Faraday Soc. 6-28.

[23 Jones, F. R. & Foreman, J. P. (2015). The response of aerospace composites to temperature and humidity in Polymer Composites in the Aerospace Industry. Woodhead Publishing, 335-369. https://doi.org/10.1016/B978-085709-523- 7.00012-8.

[24 Kabanov, B., Burstein, R. and Frumkin A. (1947). Pitting corrosion of metals – corrosion Discuss, Faraday Soc. NI. 254,12-26.

[25] Kadhim, M. G., & Albdiry, M. (2017). A critical review on corrosion and its prevention in the oilfield equipment. Journal of Petroleum Research and Study, 162-189.

[26] Kolotyrkin A. M. (2013). Pitting Corrosion of Metals. Corrosion, 19(8), 261-268. https://doi.org/10.5006/0010-9312- 19.8.261

[27] Kolotyrkin, J. M. (1963). Pitting corrosion of metals. Corrosion, 19(8). https://doi.org/10.5006/0010-9312-19.8.261

[28] Kolotyrkin, M., & Golovina, G.V. (1963). Pitting corrosion of metal, Acad. Sci. U.S.S.R. 148(106).

[29] Kumar, M., Kant, S., & Kumar, S., (2019). Corrosion behavior of wire arc sprayed Ni-based coatings in extreme environment. Materials Research Express, 6, 106427. https://doi.org/10.1088/2053-1591/ab3bd8

[30] Kumar, R., & Kumar, S. (2018). Comparative Parabolic Rate Constant and Coating Properties of Nickel, Cobalt, Iron and Metal Oxide Based Coating: A Review. I-manager's Journal on Material Sci. 6(1),45- 56. https://doi.org/10.26634/jms.6.1.14379.

[31] Kumar, R., & Kumar, S. (2018). Thermal Spray Coating Process: A Study. International Journal of Engineering Science and Research Technology, 7(3), 610-617.

[32] Kumar, R., Kumar, R., & Kumar, S. (2018). Erosion corrosion study of HVOF sprayed thermal sprayed coating on boiler tubes: a review. IJSMS. 1(3), 1-6.

[33] M. Taghavikish, N. Dutta, N. Roy Choudhury, Emerging Corrosion Inhibitors for Interfacial Coating, Coatings. 7 (2017) 217.

[34] Z. Khiati, Inhibition de la corrosion du cuivre en milieux chlorure et sulfate neutres par une nouvelle molécule dérivée de 1,2,4-triazole., (n.d.) 278.

[35] S. PAPAVINASAM__Corrosion Inhibitors // S Papavinasam Uhlig's Corrosion Handbook, 2011 Wiley Online Library

[36] M.G. Noack, EVALUATION OF CATALYZED HYDRAZINE AS AN OXYGEN SCAVENGER, Mater. Perform. 21 (1982) 26–31.

[37] D. Daoud, T. Douadi, S. Issaadi, S. Chafaa, Adsorption and corrosion inhibition of new synthesized thiophene Schiff base on mild steel X52 in HCl and H2SO4 solutions, Corrosion Science. 79 (2014) 50–58.

[38] K.F. Khaled, A. El-Maghraby, Experimental, Monte Carlo and molecular dynamics simulations to investigate corrosion inhibition of mild steel in hydrochloric acid solutions, Arabian Journal of Chemistry. 7 (2014) 319–326.

[39] X. Li, S. Deng, H. Fu, Three pyrazine derivatives as corrosion inhibitors for steel in 1.0M H2SO4 solution, Corrosion Science. 53 (2011) 3241–3247

[40] K.F. Khaled, Experimental and computational investigations of corrosion and corrosion inhibition of iron in acid solutions, Journal of Applied Electrochemistry. 41 (2011) 277–287.

[41] A.S. Fouda, H.A.A. Wahed, Corrosion inhibition of copper in HNO3 solution using thiophene and its derivatives, Arabian Journal of Chemistry. 9 (2016) S91–S99.

[42] Y. Qiang, L. Guo, S. Zhang, W. Li, S. Yu, J. Tan, Synergistic effect of tartaric acid with diaminopyridine on the corrosion inhibition of mild steel in 0.5 M HCl, Scientific Reports. 6 (2016).

[43] K.F. Khaled, The inhibition of benzimidazole derivatives on corrosion of iron in 1 M HCl solutions, Electrochimica Acta. 48 (2003) 2493–2503

[44] M. Boulkroune, A. Chibani, 2-Thiophene Carboxaldehyde as Corrosion Inhibitor for Zinc in Phosphoric Acid Solution, Chemical Science Transactions. 1 (2012) 355–364.

[45] A.B. Medrano-Solís, U. León-Silva, M.E. Nicho, 3-Thiophenemalonic acid as corrosion inhibitor of copper, Anti-Corrosion Methods and Materials. 64 (2017) 52–60.

[46] G. Gece, Theoretical evaluation of the inhibition properties of two thiophene derivatives

on corrosion of carbon steel in acidic media, Materials and Corrosion. (2012) 1-5

[47] K.F. Khaled, N.S. Abdel-Shafi, N.A. Al-Mobarak, Understanding Corrosion Inhibition of iron by 2Thiophenecarboxylic Acid Methyl Ester: Electrochemical and Computational study, Int. J. Electrochem. Sci. 7 (2012) 18.

[48] A.S. Fouda, A.A. Attia, A.A. Negm, Some Thiophene Derivatives as Corrosion Inhibitors for Carbon Steel in Hydrochloric Acid, Journal of Metallurgy. 2014 (2014) 1–15.

[49] M. Bouklah, B. Hammouti, M. Benkaddour, T. Benhadda, Thiophene derivatives as effective inhibitors for the corrosion of steel in 0.5 m H2SO4, Journal of Applied Electrochemistry. 35 (2005) 1095–1101.

[42] S. Ben Aoun, Electrochemical Impedance Spectroscopy Investigations of Steel Corrosion in Acid media in the presence of Thiophene Derivatives, International Journal of Electrochemical Science. (2016) 7343–7358.

[50] M. Bouklah, B. Hammouti, A. Aouniti, T. Benhadda, Thiophene derivatives as effective inhibitors for the corrosion of steel in 0.5M H2SO4, Progress in Organic Coatings. 49, 225-228, 2004.

[51] Galal, N.F. Atta, M.H.S. Al-Hassan, Effect of some thiophene derivatives on the electrochemical behavior of AISI 316 austenitic stainless steel in acidic solutions containing chloride ions, Materials Chemistry and Physics. 89 (2005) 38–48.

Chapter2

[52] E. Schrödinger, Phys. Rev. 28, 1049, 1926.

[53] D.Born and Oppenheimar, J.R. Ann. Phys. Rev. 84, 457, 1927.

[54] D.R. Hartree, Proc. Cambridge Philos. Soc., 24 : 89, 1928.

[55] V. Fock. Z. Phys., 61 :126, 1930.

[56] K. Haddadi, Thèse de doctorat, université Sétif, 2013.

[57] N.Richard, CEA/DAM-Direction Ile de France, 2002

[58] L.H. Thomas, Proc. Cambridge Philos. Soc. 23, 542, 1928.

[59] E. Fermi. Z. Phys, 48 : i 3, 1928.

[60] P. Hohenberg and W. Kohn, Phys. Rev. B, 136, 864, 1964.

[61] W. Kohn and L.J. Sham, Phys. Rev. A 140, 1133, 1965.

[62] P. Geerlings, F. De Proft, and W. Langenaeker, Chem. Rev., 103, 1793, 2003.

[63] S.Chabbal. Thèse de doctorat, université de Toulouse 2010.

[64] R. M. Martin, Electronic structure Basic Theory and Practical Methods, Cambridge University Press, UK 2004.

[65] E. Betranhndy, Thèse de doctorat, université Bordeaux 1, 2005.

[66] P.A.M. Dirac, Proc. Cambridge Philos. Soc, 26, 376, 1930.

[67] J.C. Slater, Phys. Rev. 81, 385, 1951.

[68] K. Schwarz, Phys. Rev. B 5, 2466, 1972.

[69] D. M. Ceperley, B. J. Alder, Phys. Rev. Lett. 45, 566, 1980.

[70] G. Ortiz et P. Ballone. Phys. Rev. B, 50(3), 1994

[71] A.D .Becke, Phys. Rev. A, 38, 3098, 1988.

[72] J. P. Perdew, "In Electronic Structure of Solids ‘91" ; Ziesche P.and Eschrig H, 1991.

[73] J. P. Perdew, Phys. Rev. B. 33, 8822, 1986.

[74] C. Lee, W. Yang, R. G. Parr, Phys. Rev. B. 37, 785, 1988.

Chapter3

[75] K. R. Ansari, M. A. Quraishi and A. Singh, Measurement, 2015, 76,136-147.

[76] R. Solmaz, E. A. Sahin, A. Doner and G. Kardas, Corros. Sci., 2011, 53, 3231-3240.

[77] H. Muster, A. E. Hughes, S. A. Furman, T. Harvey, N. Sherman, S. Hardin, P. Corrigan, D. Lau,. Scholes, P. A. White, M. Glenn, S. J. Garcia and J. M. C. Mol, Electrochim. Acta., 2009, 54, 3402-3411.

[78] C. O. Gretir, B. Mihci and G. Bereket, J. Mol. Struct., 1999, 488, 223-231.

[79] Y. Chen, Z. Chen and Y. Zhuo, Materials, 2022, 15, 4218.

[80] M. Dehdab, M. Shahraki and S. M. Habibi-Khorassani, Amino Acids, 2016, 48, 291-306.
[81] I. Lukovits, E. Kalman and F. Zucchi, Corrosion, 2001, 57, 3-8.
[82] T. Lu and F. Chen, J Comput Chem, 2012, 33, 580-592.
[83] A. El Assyry, B. Benali, B. Lakhrissi, M. El Faydy, M. Ebn Tou-hami, R. Touir, M. Touil, Res Chem Intermed. 2015, 41, 3419-3431.
[84] A. M. Al Sabagh, N. M. Nasser, A. A. Farag, M. A. Migahed, A. M. F. Eissa and T. Mahmoud, Egypt. J. Petrol., 2013, 22, 101-116.
[85] Evgueni, B., Nikolay P., & Boris S. (2004). Truncated-determinant diagrammatic monte carlo for fermions with contact interaction. Phys. Rev. 70, 15-28.

[86] Fernandes, J. S., & Montenor, F. (2015). Corrosion. Materials For Construction And Civil Engineering, 2, 679-716. [87] Giurlani & Innocenti, M. (2018). Electroplating for decorative applications: recent trends in research and development walter. Coatings, 8, 149-260.

[88] Goldstein, E. M. (1960). The Corrosion and oxidation of metals: scientific principles and practical applications. J. Chem. Educ. 37, 662-672.

[89] Hoar, T. P. (1949). Bulk metallic glasses: an overview. Trans. Faraday Soc. 45, 683-692.

[90] B.D.B. Tiu, R.C. Advincula, Reactive and Functional Polymers, 95 (2015) 25-45.